STUDY OF ATMOSPHERIC WATER BALANCE

OVER SOUTH ASIAN MONSOON REGION

(南アジアモンスーン地域における大気水収支の研究)

Venkatraman Prasanna

(ベンカットラマン　プラサンナ)

A dissertation for the degree of Doctor of Science
Department of Earth and Environmental Sciences,
Graduate School of Environmental studies,
Nagoya University.
(名古屋大学大学院環境学研究科地球環境科学専攻学位論文　博士(理学))

2008

ABSTRACT

The atmospheric water balance over different domains within the South Asian Monsoon region has been studied using moisture convergence (C) computed from JRA-25, ERA-40 and NCEP/NCAR reanalysis datasets, GPCP precipitation data (P) and evaporation (E) as a residual of these two parameters. The seasonal climatology of P, C, and E for the selected regions shows generally large contribution of E to P. The inter-annual characteristics of P, C and E over selected key domains with in the South Asian Monsoon region have also been examined for both early (JJ) and late summer (AS) monsoon periods from 1979 to 2000. The spatial and temporal characteristics of the hydrological cycle and the contribution of E and C to P are discussed in detail. One important aspect on seasonal time scale is that from dry regions of Northwest to Central and to the wettest Northeast regions, the monthly variations of E or C are large during the monsoon months specific to that region. However, the interannual variability of P over each domain is not necessarily be influenced by the same criteria like C or E, which influences the mean seasonal precipitation. It is also evident that the structure of variability for early (JJ) and late (AS) summer precipitation is different over south Asian Monsoon region. Over northwest India E dominates C on seasonal time scale, but only C contribute to interannual variability of P. Similarly, over central India C dominates E during early summer (JJ) on seasonal timescale, but E contributes higher to P variability on interannual time scale and during late summer (AS) over central India E dominates C on seasonal time scale, but C contributes higher to P variability on interannual time scale. Over northeast India, C dominates E on seasonal time scale, but only E contributes to interannual variability of P. The importances of land-atmosphere interactions over each

domain are discussed. The regionality in the mechanism of precipitation generation and its contribution to the all India summer monsoon precipitation variability are also discussed in detail. The role of evaporation on the interannual variability of precipitation is stronger over Bay of Bengal sector and the role of convergence on the interannual variability of precipitation is stronger over Arabian Sea sector.

The interannual variability of P, C and E for the northeast monsoon season (October to December) over the south Peninsular India and Sri Lanka have also been examined. The spatial and temporal characteristics of P, C and E characteristics have proved that over this region, E principally dominates during the entire monsoon months (OND). The moisture transport from the Indian Ocean sector modulates the precipitation over this region on a year-to-year basis. It has been noted that the positive northeast monsoon rainfall is associated with El-Nino coupled with positive Indian Ocean Dipole mode, but negative northeast monsoon rainfall is weakly associated only with La-Nina condition. The role of land-atmospheric interaction over the region in modulating the interannual variability of hydrological cycle has also been discussed.

CONTENTS

CHAPTER 1

INTRODUCTION

The earth's unique environment for life is determined by interactive systems comprising the atmosphere, ocean, land and then the living organisms themselves. The climate systems have shown significant changes in the past. Recently the study on climate is increasing, to understand the factors governing the climate on earth and its long-term and short-term variations. A first step towards this goal is to study the behavior of earth's climate in the recent past. A detailed knowledge of these climatic variations can serve as useful constraints on models aimed at predicting climate in the near future. Instrumental weather records, satellite observations and reanalysis provide us with useful datasets in the analysis of recent climate variations.

1.1 Observed Climate over South Asia

A variety of physiographic features like the Himalayan mountain range, Indo-Gangetic plains, the central highlands, peninsular plateau, the coastal plains, etc. defines climate over south Asia. The region has large river basins and vast areas under subtropical as well as tropical forests. Apart from these natural features, the region has large population of over a billion, leading to large-scale urbanization, industrialization, and deforestation, which have significant impact on climate of the region. The region is dominated by monsoon climate, defined by the southwesterly maritime winds that bring rainfall during the monsoon season. The northern limit of monsoon is effectively confined to Indian sub-continent due to Himalayan range, which also isolates the region

from extra-tropical influences. The region is made of diverse climatic regimes. Regional contrasts in the rainfall, with highest in the northeast (Chirapunji) to lowest in the northwestern parts (Thar Dessert) and the regional contrast in temperatures with less than 0°C over Himalayas to temperatures as high as 50°C in Rajasthan during summer, are some of the salient features.

1.2 South Asian Monsoon Climate

1.2.1 Southwest monsoon

The South Asian summer monsoon (also known as southwest monsoon) is a consequence of the thermal differences between the land and the sea. Monsoon is forced primarily due to the seasonal shifting of thermally produced planetary belts of pressure and winds under continental influences. The upper air circulation undergoes complex seasonal changes that form an essential part of the establishment of the monsoon over South Asia. The mountains and high plateaus of Central Asia facilitate the summer monsoon not only by deflecting the upper westerlies northward, but also by constituting an important heat source in the upper troposphere. Intense heating of the Tibetan Plateau deepens the low pressure over northern India, creating favourable conditions for the Asian summer monsoon to develop into a powerful air stream in the form of cross equatorial low-level jet stream (Findlater 1969).

In bringing the monsoon rains over India, the cross equatorial flow of moisture, wind as well as the evaporation over the north Indian Ocean and adjoining seas are known to be important (Cadet and Reverdin, 1981; Saha and Bavadekar, 1973). During the onset of monsoon, a strong cross equatorial low-level jet stream (LLJ) develops in

response to the large meridional pressure gradient between Asian continent and Indian Ocean regions and persists during the entire monsoon season. In the past, several studies have been made in explaining different aspects of monsoon circulation. For example, the observational and theoretical attempts were made to understand the northward migration of monsoon with seasonal and intraseasonal time scales from the equatorial Indian Ocean to the main continent (Yasunari, 1979, 1980, 1981; Sikka and Gadgil, 1980; Webster et al., 1998).

The annual rainfall amounts increase by almost three orders of magnitude from west to east across the Indian subcontinent. Devastating floods in some areas and parching droughts in some other areas in the subcontinent, occurring simultaneously is a common feature (Pant and Rupakumar, 1997). The summer monsoon contributes about 80% of the total annual rainfall in a major part of the region. The summer monsoon rainfall displays a variety of temporal and spatial variations, which is an important source of water for the country as evidenced by remarkable large-scale stability for the past, over a century of recorded data (with a coefficient of variation of 10%). Historically, above (below) average Indian monsoon rainfall in the interannual timescale has been noted to be generally associated with the cold (warm) phase of the ENSO (Rasmusson and Carpenter, 1983; Yasunari, 1990**)**.

1.2.2 Northeast monsoon

Two vital monsoon systems prevail over the Indian subcontinent, namely the summer monsoon (southwest monsoon) and northeast monsoon (also known as retreating monsoon). The southwest monsoon has been studied widely compared to the northeast monsoon. During northeast monsoon season, the heating over oceans and extensive

cooling over the continental areas facilitate the northeastward flow of winds over the Bay of Bengal and thus the moisture carried from the Bay of Bengal creates a favourable condition for northeast monsoon to develop over the south peninsular India and Sri Lanka during October to December.

The Northeast Monsoon Rainfall (NEMR) season (October, November, December) over south peninsular India and Sri Lanka is the major rainfall season over this region (Dhar and Rakhecha, 1983), which helps agricultural production in this region (Pankaj Kumar et al., 2007). NEMR received very less attention compared to summer monsoon in terms of studies in interannual variability and its teleconnections (Singh and Sontakke, 1999; Kripalani and Kumar, 2004; Pankaj Kumar et al., 2007) and over the Sri Lankan region by Suppiah (1989, 1996, 1997).

1.3 Monsoon rainfall variations

Rainfall received during the four months June through September constitutes summer monsoon rainfall. The summer monsoon or southwest monsoon season accounts for about 80% of the annual rainfall over India, followed by the winter or northeast monsoon season that accounts for about 10% of the annual rainfall. The monsoon rainfall is the main input to the Indian agriculture. Some of the important characteristics of the monsoon rainfall variability are discussed here.

1.3.1 Monsoon rainfall: Intraseasonal variations

The Indian summer monsoon exhibits pronounced intraseasonal variability on time scales ranging from a few days to more than a month. The intraseasonal oscillation of the monsoon is not periodic in nature. It has three broad bands of spectrum termed as synoptic scale variability of 6-9 days, quasi-biweekly mode of 10-20 days and

intraseasonal mode of 30-60 days (Krishnamurti and Bhalme, 1976; Krishnamurti and Ardunay, 1980; Yasunari, 1980). Most of these variabilities have been studied in almost all the monsoon elements such as pressure (Krishnamurti and Subramaniam, 1982), cross-equatorial low-level jet (Joseph et al., 2004), the surface wind speed (Goswami et al., 1998), monsoon cloudiness (Yasunari 1980, 1981; Sikka and Gadgil, 1980), monsoon rainfall (Kripalani et al., 2004), and also water vapour (Cadet and Greco., 1987).

1.3.2 Monsoon rainfall: Interannual variations

The All-India Summer Monsoon Rainfall (AISMR), which is the monsoon rainfall averaged over 306 raingauge stations in the plains over India is found to be 852 mm with a standard deviation (SD) of 85 mm and a coefficient of variability (CV) of 10%. AISMR experiences large interannual variability, with extreme cases of drought conditions (Parthasarthy et al., 1993). A year is considered a drought (flood) year if AISMR is less (greater) than the long period mean by more than 1 SD. During the period 1871-2000 there were 22 drought years and 19 flood years. Factors causing interannual variability of the monsoon rainfall are generally dominated by ENSO (Parthasarthy et al., 1987).

1.3.3 Monsoon rainfall: Decadal variations

The AISMR features practically no trend and is stable about its long period average. However, it features multi-decadal epochal variability. Epochs of above normal rainfall feature below normal interannual variability and vice versa (Pant and Rupa Kumar, 1997).

1.3.4 Monsoon rainfall: Spatial variations

During the monsoon season, the west coast of Indian Peninsula and parts of

northeast India are the regions that receive the highest amount of rainfall, while parts of northwest India receive the least amount of rainfall. Regarding spatial variability indicated by Coefficient Variance (CV), high values of (CV) are seen in low rainfall areas of Rajasthan and extreme southeast Tamil Nadu and low values of (CV) are seen over high rainfall areas of Kerala and Karnataka coast, Assam, West Bengal and northeastern states. Rainfall during the monsoon season amounts to more than 75% of the annual rainfall over most of the parts except the over Tamil Nadu, where northeast monsoon contributes to over 50% of the annual rainfall.

1.3.5 Homogeneous monsoon regions

Parthasarathy et al. (1996) have identified homogeneous regions of summer monsoon rainfall over India, based on rainfall characteristics and the associated regional and global teleconnections. These regions are: (i) Northwest India (NW); (ii) West Central India (WC); (iii) Central Northeast (CNE) India; (iv) Northeast India (NE); and (v) Peninsular India (PN). It has been found that the AISMR is positively correlated with the summer monsoon rainfall over all the homogeneous regions except that over the NE region. Further, NE is anti-correlated with all other regions, while the region WC is strongly correlated with NW and PN regions.

1.4 Aim and Scope of the Present Study

Present study is aimed at the assessment of the atmospheric water balance over the south Asian monsoon region and to understand the dynamics of variations of atmospheric water balance on seasonal to interannual timescales. The comprehensive study of atmospheric water balance is useful for the assessment of climate variations from seasonal to interannual timescales. In south Asia, agriculture forms a critical

component of the regional economy, which is mainly dependent on the monsoon rainfall. In these regions economy is highly dependent on the year-to-year variability and spatial and temporal distribution of monsoon rainfall. Hence this study examines hydrological cycle and interannual variability of precipitation over south Asia using atmospheric water balance method.

The thesis includes:

1 . Study of spatial and temporal evolution of atmospheric water balance over south Asia during early and late summer monsoon season.

2 . Estimation of precipitation variability with respect to large-scale convergence (C) and local evaporation (E) over south Asia during early and late summer monsoon season using GPCP precipitation and reanalysis datasets.

3 . Study of interannual variability of atmospheric water balance for both early and late summer and to understand the mechanism of precipitation generation and its variability

4 . Study of Interannual variability atmospheric water balance over peninsular India and Sri Lanka during northeast monsoon rainfall (NEMR) season (OND) and to understand the dynamics of precipitation variability.

CHAPTER 2

DATA

Assessment of atmospheric water balance is based on the merged rain gauge and satellite observed precipitation as well as reanalysed data products from different global climate research centers. This study uses merged rain-gauge and satellite observed precipitation data from Global Precipitation Climatology Project (GPCP) and reanalysis data products from National Center for Environmental Predictions and National Center for Atmospheric Research (NCEP/NCAR), European Center for Medium Range Weather Forecasting (ECMWF) 40 year reanalysis (ERA-40) and Japanese 25-year Re-Analysis project (JRA-25). In this chapter, a detailed account of various global and regional climate datasets is presented followed by a brief description of various reanalysis projects.

2.1 Global and Regional Climate datasets

2.1.1 Global Precipitation Data (GPCP)

A monthly precipitation dataset for both global land and oceanic areas from 1979 to present, gridded at 2.5° latitude by 2.5° longitude resolution, is prepared as GPCP version-2. The gridded data set has been constructed by merging both rain gauge based observation and satellite observation. The details of the original GPCP data are described in Adler et al. (2003). The GPCP has extended to include the TRMM and SSMI observations in the recent years. The gridded data sets made available by the GPCP forms a useful source in assessing the large-scale aspects of the precipitation. These data sets have been widely used in estimating the changes in precipitation.

2.1.2 Global land precipitation Dataset (VASClimO)

The monthly data on the global land precipitation are available since 1951 as

VASClimO (Variability Analyses of Surface Climate Observations), a 50yr precipitation climatology (Beck et al., 2000). The globally gridded monthly precipitation sums from January 1951 to December 2000 are provided in three resolutions 0.5°x0.5°, 1.0°x1.0°, and 2.5°x2.5°. This data set is an interpolated rain gauge measurement obtained from the site (*http://www.deutscherwetterdienst.de/*). VASClimO is an activity of the German Weather Service.

2.1.3 Homogeneous Indian Monthly Rainfall Data

The Indian Institute of Tropical Meteorology (IITM) has developed homogeneous all-India and regional mean monthly rainfall data sets, which are widely recognized to be highly reliable and well representative of the rainfall characteristics of the region. These are based on a uniform network of 306 stations, one from each district in the plain contiguous region over India from period 1871. The hilly regions consisting of four meteorological subdivisions of India extending into the Himalayan mountain range have not been considered in view of the meager rain-gauge network and low areal representation of a rain gauge in the hilly area. Two island subdivisions far away from mainland have not been included. The contiguous area covered by the network of 306 stations over 29 meteorological subdivisions measures about 2,880,000 sq km., which is about 90% of the total area of the country. The all-India regional and sub-divisional mean monthly rainfall data sets (IITM-IMR data) for the period 1871-1999 are available at (http://www.tropmet.res.in/).

2.1.4 Global Sea surface Temperature

The study uses global monthly sea surface temperature data gridded at 1.0°x1.0° resolution from 1982-2005 NOAA_OI_SST_V2 (NOAA Optimum Interpolated SST dataset) (Reynolds et al., 2002). NOAA_OI_SST_V2 obtained from the web site

(http://www.cdc.noaa.gov/).

2.2 Global Reanalysis Climate datasets

2.2.1 Global Zonal and Meridional Tropospheric variables

Daily upper level winds, specific humidity, geopotential height, surface winds, surface level specific humidity and sea level pressure at a resolution of 2.5°x2.5° from NCEP/NCAR reanalysis (Kalnay et al. 1996) were obtained for the period 1979-2005 from the web site (http://www.cdc.noaa.gov/).

Six hourly upper level variables for ERA-40 reanalysis dataset (Uppala et al. 2005) for the period 1979-2000 at a resolution of 2.5°x2.5° were obtained from the website (*http://data.ecmwf.int/data/*).

Similarly, six hourly upper level variables for JRA-25 dataset (Onogi et al., 2005) for the period 1979-2000 at a resolution of 1.25°x1.25° were obtained from the website (http://jra.kishou.go.jp).

2.3 Brief description of Reanalysis projects

2.3.1 NCEP/NCAR reanalysis project

The NCEP/NCAR reanalysis project is a joint project between (NCEP, formerly "NMC") and NCAR. The goal of this joint effort is to produce new atmospheric analyses using historical data (1948 onwards) and as well to produce analyses of the current atmospheric state (Climate Data Assimilation System, CDAS). The resolution of the global reanalysis model is T62 (209 km) with 28 vertical sigma levels. There are over 80 different variables, (including geopotential height, temperature, relative humidity, horizontal wind components, etc.) in several different coordinate systems, such as 17-pressure level on 2.5x2.5 degree grids, 28-sigma level on 192x94 Gaussian grids, and 11

isentropic levels on 2.5x2.5 degree grid. The basic idea of the Reanalysis Project is to use a frozen state-of-the-art analysis/forecast system and perform data assimilation using past data from 1957 to the present (reanalysis). Moreover, the same frozen analysis/forecast system are to be continued to perform data assimilation into the future (CDAS), so that climate researchers can assess whether the current climate anomalies are significant when compared to a long reanalysis without changes in the data assimilation system. The NCEP/NCAR reanalysis data is a research-quality data set suitable short and long-term climate research. A state-of-the-art data assimilation is used. Observations from land surface, ship, rawinsonde, pibal, aircraft, satellite and other data are quality controlled and assimilated into the model, the model/data assimilation procedure has remained essentially unchanged during the project; data assimilation includes SSM/I surface winds and tropospheric and stratospheric temperatures retrieved from TOVS (Kalnay, 1996).

2.3.2 ERA-40 reanalysis project

The objectives of the European Centre for Medium-Range Weather Forecasts (ERA-40) project are to produce and promote use of a comprehensive set of global analyses describing the state of the atmosphere, land and ocean-wave conditions from mid-1957 to August 2002. The three dimensional variational technique has been applied using the T159L60 version of the Integrated Forecasting System to produce the analyses every six hours. The data has been produced in three streams, defined by the availability of observational data for each given period: Stream-1 (1987-2002), includes observation types (like TOVS, SSM/I, ERS, ATOVS and CMV), Stream-2 (1957-1972) includes Pre-satellite, old observation types only and Stream-3 (1972-1988) includes only some satellite observation type (VTPR,TOVS and CMW). Analysis involving comprehensive use of satellite data, started from the early Vertical Temperature Profile Radiometer data in 1972, then later TOVS, SSM/I, ERS and ATOVS data are included. Cloud Motion

Winds are used from 1979 onwards.

2.3.3 JRA-25 reanalysis project

Japanese 25-year Re-Analysis project (JRA-25) is a joint research project with the Central Research Institute of Electric Power Industry (CRIEPI) of Japan since April 2001 to make a long-term (about 26 years from 1979 to 2004) and high quality reanalysis dataset. The major objective of the project is to make a fundamental dataset for dynamical seasonal prediction, accurate climate system monitoring, and climate system studies. Production of JRA-25 was completed in March 2006. Dataset can be downloaded from their site (http://jra.kishou.go.jp). The global forecast model used for JRA-25 has the resolution of spectral T106 (equivalent to horizontal grid size around 110km) and 40 vertical layers of the top level at 0.4hPa, and the data assimilation scheme is 3-dimensional variational (3DVAR) system. JRA-25 is the first reanalysis to use wind profile retrievals surrounding tropical cyclones (TCR), SSM/I snow coverage, digitized Chinese snow depth data, reprocessed GMS-AMV and daily COBE SST and sea ice data as boundary forcing (Onogi et al., 2005).

CHAPTER 3

METHODOLOGY

The methodology to obtain the moisture convergence on monthly scale south Asia using daily and six hourly reanalysis products from NCEP/NCAR, ERA-40 and JRA-25 are discussed in detail in this chapter.

Water budget is the most fundamental aspect of the hydrological cycle. Traditionally, evapotranspiration has been estimated using observational data at ground surface. Currently, there are many studies to estimate evapotranspiration over large spatial scales using satellite remote sensing. However, it is still difficult to obtain very reliable estimates. On the other hand, water balance estimation using atmospheric data, namely the atmospheric water balance method, is easier to apply due to the availability of high-resolution atmospheric data. A simple schematic diagram to understand the atmospheric water balance is shown in (Fig. 3.1).

Following the seminal works on global atmospheric water balance studies (Trenberth, 1991; Oki et al., 1995; Trenberth and Guillemot, 1998; Trenberth, 1999), we have attempted to understand the atmospheric water balance over South Asia using objectively reanalysed gridded four-dimensional datasets (like NCEP/NCAR and ERA-40, JRA-25) and observed precipitation (P) from GPCP.

3.1 Method of Analysis

The atmospheric water budget equation can be written as (Peixoto and Oort 1992),

$$< \partial W/ \partial t > + < \nabla \quad . Q > = < E - P > \quad \text{..... (1)}$$

Where (***P)*** is precipitation, (***E)*** is evaporation, and angled brackets denote the area average, precipitable water content (***W***), vertically integrated moisture flux vector (**Q**), and its divergence ($\nabla \cdot \mathbf{Q}$).

On longer timescales like monthly or seasonal, under near equilibrium conditions, the time change of local available precipitable water content is negligible compared to the variations of large-scale convergence and evaporation (Oki et al., 1995; Trenberth, 1999). We approximate,

$$< \partial W / \partial t > \sim 0 \quad \text{.....(2)}$$

There fore we can approximately write,

$$P \sim C + E \quad \text{.....(3)}$$

Vertically integrated moisture flux vector (**Q**) is given by,

$$Q = 1/g \int_{Pt}^{Ps} qvdp \quad \text{.....(4)}$$

Where q is the specific humidity, v is the horizontal wind vector, Ps is the pressure at surface level and Pt is the pressure at the top of the atmosphere, g is gravitational acceleration. Vertical integration is performed from ground level (surface pressure level) to 300 hPa for the standard atmospheric pressure level (1000, 925, 850, 700, 600, 500, 400, 300 hPa). We can neglect pressure levels above 300 hPa, as the specific humidity above this level is negligible. The moisture flux divergence that is the second term in the left-hand side of equation (1) and the vertically integrated moisture fluxes are computed using the linear grids.

3.2 Computed large scale Convergence from reanalyses

The large-scale moisture convergence computed from three different reanalyses are shown in Fig. 3.2a, b, c.

The large-scale convergences computed from different reanalysis dataset differ considerably, because the data assimilation may vary among reanalyses over a specific region and over data sparse regions, the data is filled with the first guess, so regions with data sparse like oceans are completely model dependent. The regions with dense observations will have high reliability, for example over continental regions.

Some of the observations made based on this study and from the expert references, that the ERA-40 has problems over the regions close to tropics. The ERA-40 has estimated strong convergence over oceans and strong divergence over land. Hagemann et al. (2005) also found that the hydrological cycle over land is generally improved in ERA-40 compared to the previous ERA-15, but found P-E over the ocean is positive (and not negative as it should be) and quoted, the fact that the global water balance is not only unbalanced, the evapotranspiration over land is overestimated for many catchments, and finally suggested that conclusions drawn for hydrological trends should be taken with great care.

Some Problems and deficiencies of the column integrated water vapour highlighted by (Trenberth et al., 2005) are, both NCEP reanalyses are deficient over Ocean (NCEP-1 and NCEP-2): the mean, the variability and trends and the structures of variability are not realistic, stems from the lack of assimilation of water vapour information from satellites into the analyses and model biases. JRA-25 dataset appears to be quite reliable over land and where dense concentrations of radiosondes exist. Hence, instead of relying on one dataset, we have tried to exploit different dataset to reassure our confidence on the calculated moisture convergence (C).

CHAPTER 4

TIME-SPACE CHARACTERISTICS OF SEASONAL AND INTERANNUAL VARIATIONS OF ATMOSPHERIC WATER BALANCE OVER SOUTH ASIA

4.1. Overview

The motivation of the present study is to understand the nature of the large-scale water balance over south Asia on seasonal and interannual timescales. Moreover it is needed to facilitate the understanding of hydro meteorological processes in different regional domains within the south Asian monsoon region. For this purpose, the space-time characteristics of seasonal and interannual variations of Precipitation (P), Moisture Convergence (C) and Evaporation (E) during the period, starting from 1979 up to 2000 has been studied in detail. A particular attention has been paid to understand, where does the precipitation (P) come, i.e., from large-scale moisture convergence (C) due to atmospheric circulation, and/or from Evaporation (E) from the surface?

Why atmospheric water balance analysis is required here? Because, the Indian summer monsoon or the south Asian Monsoon has long been conventionally studied as, the rainfall averaged over the entire country (India) and summed over four months as a single seasonal mean index (JJAS) or simply denoted by AISMR for characterizing wet or dry condition. So analysis based on water balance helps us to clearly establish the differences within the season and among the regions over the south Asian monsoon

domain. Moreover, the origin of (P) and relationship with C & E and its variability on seasonal and interannual scale can be captured clearly.

Following the seminal works on global water budget studies (Trenberth, 1991; Oki et al., 1995; Trenberth and Guillemot, 1998; Trenberth, 1999), we have attempted to understand the atmospheric water balance over South Asia. Objectively reanalysed gridded four-dimensional datasets (like JRA-25, ERA-40 and NCEP/NCAR) give us a great opportunity to study water balance on global and regional scales. Though there are physical constraints in the closed water budget calculation and may be imperfect to use observed precipitation (P) to close the reanalyses water budget, it provides an opportunity to obtain less observed variable evaporation (E) at each grid point on regional and global scale through the balance. Since the reanalysis simulated evaporation is heavily model dependent and the simulated precipitation is constrained by the model's parameterization schemes, we have tried to utilize the advantage of monthly observed precipitation (P) to find the residual evaporation.

There are a few previous regional studies which uses observed precipitation to obtain atmospheric water balance (Oki et al., 1995; Fukutomi et al., 2003; Marengo, 2005). The evaporation obtained as a residual from the water balance method suffers from substantial errors; the accuracy of (E) depends on the accuracy of observed (P) as well as the accuracy of computed (C). Oki et al. (1995) applied the global atmospheric water balance analysis to study the water balance over the Chao Phraya river basin and estimated a much better evapotranspiration on monthly timescales than the ECMWF operational model obtained (E), using the same assimilated datasets and observed values of precipitation over the basin catchment area. Fukutomi et al. (2003) studied interannual variability of summer water balance over three major river basins (Lena, Yennisey and Ob) using observed (CMAP) precipitation, runoff datasets and convergence computed

from NCEP-II reanalysis dataset in the water budget equation. Marengo (2005) studied spatio-temporal variability of the Amazon River basin water budget using NCEP/NCAR reanalysis and observed gridded gauge precipitation dataset and compared with other datasets like GPCP, CRU. In this paper, we try to exploit the advantages of atmospheric water budget analysis for understanding precipitation generation over different sub-domains within Indian monsoon region using GPCP dataset and major reanalysis datasets.

Ailikun and Yasunari (2001) noted that the June (J) and July, August, September (JAS) rainfalls are characteristically different from each other over the Indian monsoon domain. They noticed that the early period (June) is strongly influenced by anomalous state of ENSO in the previous winter, whereas the mid-late period (July-August-September) is related to the anomalous state of ENSO in the following winter rather than the previous winter. Kawamura et al. (2005) also emphasized that, the monsoon-ENSO relationship was strong in late summer (AS) over central and northwest India before 1970s, but in the recent decades it has shifted to early summer (JJ) over northeast India and argued that the change in Monsoon-ENSO relationship based on all India summer monsoon rainfall (AISMR) represents a change in the dominance of spatial correlation pattern, from Northwest to Northeast after the late 1970s. Thus, as suggested by Ailikun and Yasunari (2001) as well as Kawamura et al. (2005), the summer monsoon period (JJAS) has been judiciously divided into early summer (JJ) and late summer (AS) for assessing the interannual variability of precipitation and atmospheric water budget components in the summer monsoon season. In this paper, we basically stress the time-space characteristics of water balance components on seasonal timescale as well as its variability on interannaul timescale. Further we discuss the regional contrast of the water budget components and also how the budget components control the precipitation generation and its variability over each domain.

The structure of this chapter is as follows. Section 4.2 describes the datasets and the computational procedures used in this study. In any analysis of geophysical parameters, the accuracy of the desired results depends on the method employed and the accuracy of the data sets used in the analysis, hence in this section the data products used and the methods employed for the interpretation of the results have been discussed in brief. Section 4.3 discusses spatial correlations of AISMR with monsoon rainfall (JJAS), early summer rainfall (JJ) and late summer rainfall (AS) periods. Section 4.4 presents a discussion of spatial differences between wet and dry years. In Section 4.5, we document the basic features of the monthly annual cycle of water balance components (E, P and C) and seasonal march of precipitation over the selected domains. Section 4.6 presents the interannual variability of precipitation and atmospheric water balance components. Section 4.7 discusses the aspect of regional variability of atmospheric water balance. In Section 4.8, the main conclusions and discussions are addressed.

4.2. Data and Method of Analysis

Water budget calculations and data analyses were performed for the 22-yr period from January 1979 through December 2000, as the reliable precipitation data over both land and ocean are available from 1979. We have utilized GPCP precipitation estimate for both land and ocean as the precipitation estimate over land areas are quite realistic in GPCP. The advantage of GPCP dataset over other land based dataset is the blending of various observational datasets like gauge precipitation, infrared precipitation estimates and precipitation estimates from microwave sensors (Adler et al. 2003).

Generally, we adopted our results from JRA-25 reanalysis dataset for discussion and compared our results with the ERA-40 reanalysis dataset and NCEP/NCAR

reanalysis dataset where ever necessary. JRA-25 reanalysis dataset has high spatial resolution compared to the other reanalysis datasets. Moreover, good correlations between P and C are noted over all the major study domains, particularly with CEN where both P and C are expected most reliable because of high density of original station data (Table-4.1). Differences in the vertically integrated precipitable water between NCEP/NCAR and ERA-40 and SSMI datasets have already been discussed in detail and found substantial problems in the low latitudes in the ERA-40 dataset (Trenberth et al. 2005). Moreover, Graversen et al. (2007) have also noted atmospheric mass transport inconsistencies in ERA-40 reanalysis. Spurious mass fluxes lead to considerable errors when zonally and vertically integrated quantities are considered. A detailed study on atmospheric hydrological cycle in the ERA-40 datasets has been dealt by Hagemann et al. (2005) and found considerable bias over land and oceans. So we basically stress more on the results obtained from JRA-25 reanalysis dataset and compare it with ERA-40 and NCEP/NCAR reanalysis datasets. All the reanalysis results agree with one another over the regions, where higher concentrations of reliable observations are available (e.g., CEN domain).

However for brevity, the study area over the south Asian monsoon region has been selected as six sub domains, but discussions are restricted to only a few major sub domains like (NWI, CEN, NEI and BOB) (Fig. 4.1b), the mean JJAS precipitation over south Asia is shown in Fig. 4.1a. The regions like driest, wettest, transition between dry and wet and oceans are arbitrarily selected and analyzed for space-time features in detail. On monthly time scales, we can approximate $P \sim C + E$, by neglecting local time change. Convergence has been computed from the vertically integrated moisture fluxes and (E) is obtained as a residual from (P) and (C), $E \sim P - C$. The mean monthly contribution of evaporation (E) or convergence (C) to precipitation (P) and the year-to-year change in

evaporation (ΔE) or convergence (ΔC) to precipitation (ΔP) are used to understand the seasonal and interannual variability respectively over different domains of south Asian monsoon region, while interpreting the results caution has been exercised on the sign of convergence and divergence. Note that the sign of convergence has been reversed in this paper for convenience.

4.3. Monsoon Indices

The all India summer monsoon rainfall index has been a widely used index for discussing strength of the Asian summer monsoon and Indian monsoon in particular (Parthasarathy et al. 1995). To examine the differences in the representation of AISMR in the early and late summer and the associated regional differences, the AISMR index has been correlated with spatial precipitation for entire summer, early summer and late summer seasons. The correlation between the AISMR index and land gridded precipitation (VASClimO) for the entire summer (JJAS), early summer (JJ) and late summer (AS) seasons are shown in Fig. 4.2 a, b, c. The highly significant correlations are seen over the northwest and central Indian regions during JJAS (Fig. 4.2a). Similarly the significant correlations are also confined to northwest India and central India during the early summer (JJ) (Fig. 4.2b). During the late summer monsoon period (AS), the significant positive correlations are again confined to central and western India and a few pockets of significant negative correlation are seen over Bangladesh region (Fig. 4.2c). These results suggest that the late summer regional rainfall (AS) over the northeast India has a non-negligible negative correlation with the AISMR variability. The basic purpose of preparing the spatial correlation map between summer monsoon precipitation and AISMR index is to highlight the regional differences in the precipitation variability

among the selected sub-domains on interannual timescales.

4.4. Difference in large-scale anomalies of (P) and (C) between wet and dry years

AISMR from June to September is shown in Fig. 4.3. AISMR has been considered to be stable with less trend and large interannual variability compared to other regions (Pant and Rupakumar, 1997). The interannual precipitation anomalies are shown as standardised anomalies from 1979-2000. The AISMR mean is given by 830 mm for 22-year period (1979-2000) and the interannual standard deviation of AISMR for 22-year period is given by 75.4 mm. The wet and dry years are identified by a departure of more than one standard deviation from the mean precipitation for the respective years. The wet years are identified as 1983, 1988, 1990, 1994 and the dry years are identified as 1979, 1982, 1986 and 1987 respectively.

To study spatial pattern of anomalies of the summer monsoon precipitation over the whole of India, the composite map for wet and dry years are prepared (wet-dry) from the interannual standard deviations of AISMR (JJAS) (Fig. 4.3). The difference composite (wet-dry) is made from four anomalous wet years and four anomalous dry years during 1979-2000. Figure 4.4 represents the composite difference of JJAS (Fig. 4.4a), JJ (Fig. 4.4b) and AS (Fig. 4.4c) between the wet and dry years of AISMR.

We notice large positive anomalies of precipitation (Fig. 4.4a) over most part of Indian region for the entire monsoon period (JJAS) and a small pocket of negative anomaly over the northeast India. Similar composite only for the (JJ) early monsoon period is also made, large positive anomalies of precipitation envelopes the entire Indian region (Fig. 4.4b). During the late summer monsoon season (AS), however, the precipitation anomaly becomes negative (large) over the northeast Indian regions (Fig.

4.4c). Thus, positive rainfall anomalies over the entire subcontinent during the early summer (JJ) do not persist until late summer (AS) even during wet years, but large negative rainfall anomalies appear in late summer (AS) over northeast India. Such appearance of large negative rainfall anomalies over the northeast India (NEI) in the wet years prevailing over most part of the subcontinent, establishes the inverse relationship that exists between NEI and the rest of the subcontinent particularly for late summer (AS) months. A significant test of difference (two tailed t-test) has been performed for early and late summer precipitation (Fig. 4.4d, e). The regions of significant difference are confined to high precipitation regions of northeast and west coast of India for both early and late summer precipitation (Fig. 4.4d, e). The t-test values above 3.71 (99%level) are darkly shaded and t-test values above 2.48 (95% level) are lightly shaded.

Thus, the over all spatial patterns of the JJAS precipitation anomalies for (wet-dry) fail to capture the large-scale difference, due to the different situation of the early monsoon season (JJ) and the late monsoon season (AS). Thus instead of using (JJAS) as one season for interannual studies, we can split it into early (JJ) and late (AS) monsoon seasons. The atmospheric water budget on monthly, seasonal, interannual time scales and the associated regionality is presented in the following sections.

4.5. Monthly annual cycle and interannual variation of moisture convergence (C) among reanalysis datasets

To elucidate how we exploited the advantages of all the major reanalysis datasets. Here we try to show, the agreement or departure among datasets over different domains. Figure 4.5 and 4.6 shows the monthly mean cycle of computed convergence (C) and interannual variability of computed convergence (ΔC) from all the three major reanalysis datasets over the selected domains. The similarity in the monthly cycle and

differences among the reanalysis over each domain is evident from the graphs (figure 4.5). Generally, the reanalysis results are in good agreement over (CEN) land domain, large discrepancies are noted over south peninsular Indian domain and Oceans. The computed convergence (C) over CEN and NEI are quite good compared to other domains. Over most of the domains the computed convergence (C) from JRA-25 reanalysis exceeds both ERA-40 and NCEP/NCAR. JRA-25 has a unique advantage over the other two datasets because of its relatively high resolution for water budget analysis and also good correlations between P and C are noted over all the major study domains (Table-4.1). So, we believe that JRA-25 dataset could be a better dataset for regions with high orography (like NEI) due to the use of high resolution model and as well as improvements in data assimilation while generating reanalysis dataset compared to the other two reanalysis datasets. Figure 4.6 shows the interannual variability of computed convergence (ΔC) over NWI, CEN and NEI. The computed convergence (C) over NWI has large discrepancies among reanalysis datasets, while the (ΔC) from JRA-25 and NCEP/NCAR results are comparable to each other in their magnitudes in early summer and late summer (Figs. 4.6a, 4.6b). Over CEN domain all the reanalysis results have comparable magnitude of C (Fig. 4.5c) and ΔC (Figs. 4.6c, 4.6d). Whereas over NEI domain, the early summer shows large deviations of C and ΔC (Fig. 4.6e), but the deviations of C and ΔC are less during late summer (Fig. 4.6f). Therefore, the land domains considered in this study have shown reasonable agreement among the available major reanalysis datasets.

4.5.1. Monthly annual cycle of atmospheric water budgets

The monthly mean annual cycle of (P), (E) and (C) over the six sub domains using JRA-25 reanalysis results are shown in Fig. 4.7. Before explaining the relative contribution of (C) or (E) to precipitation (P) on monthly scale, let us briefly explain the

seasonal march of precipitation over the different domains. Monsoon months are identified for each sub domain when the precipitation exceeds 3mm/day and are demarcated by dotted lines.

4.5.1.1. Seasonal march of (P)

Figure 4.7a shows P, C and E for the northwest India (NWI) domain, the driest region of the Indian subcontinent. The monsoon rains start from June, and precipitation attains peak in July. July month gets a decent 5 mm/day precipitation. Though monsoon continues till the end of September, the precipitation amount is very low. We can see a sudden increase of precipitation as the monsoon month arrives and between the pre-monsoon months precipitation amount was nearly 0 mm/day. Monsoon months are demarcated by dotted lines where precipitation exceeds 3mm/day.

In contrast, over Northeast India (NEI) (Fig. 4.7b), the wettest region of the Indian subcontinent, precipitation amount gradually increases from April and extends till the end of September, i.e., the rainy period over NEI is longer in the subcontinent of around 6 months duration, but considerable amount of precipitation is realized within the period of JJAS.

Over the Central India (CEN) (Fig. 4.7c), the precipitation increases suddenly during the month of May and June, from around 1 mm/day to 5 mm/day. Precipitation reaches its peak during July (8 mm/day) and the peak values are maintained until August and then precipitation falls gradually there after, but significant precipitation is confined to the four months of summer monsoon (JJAS).

Peninsular India (PEN) (Fig. 4.7d) exhibits a long rainy season; relatively low magnitude of precipitation compared to NEI region. The precipitation amount gradually increases from May above 3mm/day and attains a peak in the month of June and sustains the peak till July and slowly falls in the successive months, but does not fall completely

and second peak-like pattern appears near October-November. This is because of the precipitation from northeast monsoon, mainly due to reversal of winds from southwesterly to northeasterly. The moisture carried from the Bay of Bengal through northeasterly during October-December brings about precipitation over the peninsular India as the northeast monsoon. The northeast monsoon precipitation (October-December) is especially significant over the state of Tamil Nadu (Dhar and Rakhecha, 1983).

Over the Arabian Sea (ARS) (Fig. 4.7e), the active monsoon precipitation period is very short compared to other domains. The precipitation peak is seen during June, around 5 mm/day.

Over the Bay of Bengal (BOB) (Fig. 4.7f), the seasonal march is quite similar to the Peninsular India (PEN) region; the precipitation is prolonged for a longer duration, starting from May till November. The precipitation peak during June around 8 mm/day gets sustained in its vigour until October with the precipitation amount roughly 5 mm/day, and a small peak-like groove appears in November due to the northeast monsoon activity over the Bay of Bengal.

4.5.1.2. Seasonal contribution of (C) and (E) to (P)

Over NWI region, the precipitation during the monsoon months (JJA) is predominantly due to high evaporation (Fig. 4.7a) shown as box [E], where (E) exceeds (C) throughout the summer season (P ~ E). The higher evaporation over NWI domain is brought out in all the reanalysis results i.e., (P < E) and the magnitude of residual E is greatest in the ERA-40 reanalysis dataset (Figure not shown), while NCEP/NCAR results over NWI resemble JRA-25 results, but E exceeds P i.e., (P < E) ((Figures not shown).

Over the NEI region (Fig. 4.7b), the heavy precipitation during monsoon months

(JJAS) is mainly due to the influence of active moisture convergence, (C) exceeds (E) i.e., (C > E) and (P ~ C) during the entire monsoon months (JJAS), shown as box [C], which slightly differs with the ERA-40 reanalysis but NCEP/NCAR reanalysis shows (C) slightly exceeds (E) i.e., (C ~ E) during peak monsoon months (Figures not shown).

Over the CEN region, the monsoon rains are contributed equally by moisture convergence and evaporation during monsoon months (Fig. 4.7c) with early summer period (JJ) dominated by convergence shown as the box [C] followed by evaporation in the late summer period (AS) shown as the box [E]. The August and September months rainfall over the central India are very much influenced by higher evaporation shown as the box [E], i.e., (C) > (E) during early summer and (E) > (C) during late summer (Fig. 4.7c). The dominance of convergence during early summer has been brought out by the other two reanalysis datasets too. During early summer (C) > (E) and (E) > (C) during late summer from NCEP/NCAR and ERA-40 agrees well with JRA-25 results (Figures not shown).

The result suggests that the moisture availability during the later period of the monsoon months facilitated by the early summer (JJ) precipitation may aid in higher evaporation during the latter months and thus the structure of precipitation generation during early and late summer are different over this region.

Rainfall over PEN region (Fig. 4.7d) during monsoon months is favoured by strong convergence through out the season shown as the box [C]. Similarly over ARS region, convergence is higher (shown as the box [C]) (Fig. 4.7e) during the rainy season of the year. Convergence exceeds evaporation, i.e., (C) > (E) during monsoon months.

Over the BOB region, convergence is dominant throughout the (JJAS) season (shown as the box [C]) (Fig. 4.7f). Convergence approximately equals precipitation, i.e., (P) ~ (C) during monsoon months, which has been brought out in the NCEP/NCAR

reanalysis too (Figure not shown); whereas in ERA-40 (Figure not shown), evaporation is higher than convergence in magnitude during JJAS, suggesting both evaporation and convergence contribute to precipitation during the monsoon months.

4.6. Interannual variation of atmospheric water budgets

To study the precipitation variability on interannual time scale, the interannual variations of water budget components are plotted for both early and late summer for each domain. The correlation coefficient (CC) between ΔP and ΔC, ΔP and ΔE are used to understand the relationship of these three components in the interannual variability. The CC's are examined to know how they are related and how they differ from early to late summer period. Since E is obtained as a residual from P and C, E contains the P signature when C does not vary, so care has been taken while interpreting correlation between P and E. For understanding the interannual variability of P, C and E over domains like NWI, NEI and CEN only land grid points are considered for area average.

Though the contribution of evaporation to mean seasonal precipitation is high over the Northwest Indian region both in early and late summer monsoon period, the correlation between (ΔP) and (ΔC) are 0.86 and 0.81 (exceeds 95% significant level) for early and late summer, respectively, and correlation between (ΔP) and (ΔE) are 0.05 and 0.22 (Figs. 4.8a and 4.8b). The results from ERA-40 also supports the conclusion from JRA-25 (Figure not shown) but NCEP/NCAR (Figure not shown) is slightly different from JRA-25 results and shows significant correlation between (ΔP) and (ΔE), Since (E) is obtained as a residual and one has to be cautious while interpreting results based on residual component in the NCEP/NCAR case. Therefore (ΔC) affects the year-to-year variability of (P) over NWI monsoon region.

NEI monsoon region shows correlation coefficients of 0.49 and 0.54 between (ΔP) and (ΔC) (at just above 95% of significant level) for early and late summer respectively, JJ (0.63) and AS (0.59) between (ΔP) and (ΔE) (above 95% of significant level) respectively (Figs. 4.8e and 4.8f). These results suggest that evaporation also partly play a role in modulating the precipitation anomalies, which are well supported by both ERA-40 and NCEP/NCAR results. The correlation coefficients of 0.66 and 0.35 between (ΔP) and (ΔC) (at just above and below 95% of significant level) for early and late summer respectively, 0.55 and 0.69 between (ΔP) and (ΔE) (above 95% of significant level) for early and late summer respectively in case of ERA-40 reanalysis (Figure not shown). The correlation coefficients of 0.58 and 0.40 between (ΔP) and (ΔC) (at just above and below 95% of significant level) for early and late summer respectively, 0.81 and 0.78 between (ΔP) and (ΔE) (above 95% of significant level) for early and late summer respectively in case of NCEP/NCAR reanalysis (Figure not shown).

Similarly, over the CEN region precipitation (ΔP) is highly correlated with convergence (ΔC) (above 95% of significant level) for both early and late summer monsoon periods (Figs. 4.8c, 4.8d) and the CC between ΔP vs. ΔE in CEN considerably changes from JJ (0.41) to AS (0.08) suggesting that though C > E in the early summer and E > C in the late summer, while the interannual variability for respective seasons are reversed, i.e., ΔE contributes to ΔP for early summer and ΔC contributes to ΔP for late summer respectively. This has been reinstated in all the reanalysis results, i.e., the CC between ΔP vs. ΔE in CEN for ERA-40 changes from JJ (0.65) to AS (0.28) (Figure not shown) and also for NCEP/NCAR changes from JJ (0.78) to AS (0.38) (Figure not shown). ΔP vs. ΔE is above 95% of significant level during early summer in all the reanalysis results, but ΔE looses its significance during the late summer.

One important point to be noted here is that, over all the domains except over NEI,

the correlation coefficient (CC) between (ΔP) and (ΔC) is higher compared to (ΔP) and (ΔE), while over NEI that between (ΔP) and (ΔE) is high in both early and late summer. This suggests that the (P) variability over NEI during the summer is less dependent on large-scale convergence (C), though P at NEI is less reliable due to orography and a data sparse area. The results from ERA-40 and NCEP/NCAR are also in agreement with JRA-25 results over most of the domains.

In contrast, over the BOB monsoon region, though the active convergence during the monsoon months contribute to higher mean seasonal precipitation, the year-to-year variability of precipitation is not completely dependent on moisture convergence (similar to NEI domain), which is evident from the poor correlation between precipitation (ΔP) and convergence (ΔC) at -0.47 and 0 for early and late summer respectively (Figs. 4.9a and 4.9b) and between (ΔP) and (ΔE) JJ (0.51) and AS(0.58) (above 95% of significant level) respectively (Figs. 4.9a and 4.9b). These results suggest that evaporation plays a key role in modulating the precipitation anomalies over BOB. Still the quality of observed P and computed C over oceans are not reliable as they are data sparse regions, so the results based on JRA-25 reanalysis is only tentative.

Over the PEN monsoon domain, the correlation between (ΔP) and (ΔC) are 0.46 and 0.73 (95% significant level) for early and late summer, respectively, and correlation between (ΔP) and (ΔE) are 0.21 and 0.32 (Figs. 4.9c and 4.9d). The results from ERA-40 supports the conclusion from JRA-25 and the correlation between (ΔP) and (ΔC) are 0.62 and 0.77 (95% significant level) (Figure not shown). The NCEP/NCAR (Figure not shown) also supports JRA-25 results and the correlation between (ΔP) and (ΔC) are 0.56 and 0.77 (95% significant level). Therefore (ΔC) affects the year-to-year variability of (P) over PEN monsoon region.

Similarly, over the ARS monsoon domain, the correlation between (ΔP) and (ΔC)

are 0.41 and 0.55 (95% significant level) for early and late summer, respectively, and correlation between (ΔP) and (ΔE) are 0.31 and -0.22 (Figs. 4.9e and 4.9f). Therefore (ΔC) affects the year-to-year variability of (P) over ARS monsoon region. The results from ERA-40 supports the conclusion from JRA-25 and the correlation between (ΔP) and (ΔC) are 0.78 and 0.69 (95% significant level) (Figure not shown). The NCEP/NCAR (Figure not shown) also supports JRA-25 results and the correlation between (ΔP) and (ΔC) are 0.63 and 0.79 (95% significant level). Still the quality of observed P and computed C over oceans are not reliable as they are data sparse regions.

4.7. Regional variability in atmospheric water budget

Indian summer monsoon exhibits a large variety of spatial and temporal variability. In this section we discuss the characteristics of atmospheric circulation, moisture transport responsible for precipitation generation during early and late summer among the selected domains. Precipitation (P), large-scale convergence (C), winds, moisture transport vectors and evaporation (E) are regressed with the averaged GPCP precipitation index over each domain in order to understand the structure of (P) variability, over the respective domains. A test of local statistical significance for spatial correlation coefficient was performed using standard t-test for plotting above 95% significance level.

Figure 4.10a, b shows GPCP precipitation and 850hpa winds regressed with NWI domain averaged GPCP precipitation for early and late summer, respectively. During early summer (JJ) (Fig. 4.10a), the regression pattern reveals that the precipitation anomalies over NWI are strongly associated with local (P) and moderately associated with (P) along the west coast, Arabian Sea and the Bay of Bengal region, where as during

late summer (AS) (Fig. 4.10b) the precipitation anomalies have profound effect only over the west coast and north west India. The precipitation during late summer (AS) over NWI is negatively associated with northeast India (NEI) precipitation. The precipitation during early summer (JJ) are generally caused by the disturbances from the Bay of Bengal sector (associated with monsoon trough) and strong convergence over Arabian sea sector, the positive precipitation anomalies over NWI are coupled with the cyclonic circulations over Arabian sea and the land regions, especially over central India and near the head bay (Fig. 4.10a,c). During late summer (AS), the cyclonic circulation is confined to the Arabian Sea sector and the regression coefficients are confined only over northwest India. Therefore, the positive precipitation anomalies over NWI for late summer (AS) are coupled with cyclonic circulation over Arabian Sea only and strong moisture transport vectors predominantly originate from Arabian Sea sector (Fig. 4.10b,d).

From the regressed pattern of (E), one can notice no role of evaporation during the early summer and late summer over NWI to (P) variability (Fig. 4.10e, f). The role of (E) in modulating the precipitation anomalies over NWI may not be very high over land as P itself is small, but the evaporation from the adjacent oceanic regions may partly play as a source. So, (ΔC) plays a major role in the interannual variability over northwest India in early summer (JJ) and also in late summer (AS).

Figure 4.11a,b shows the regressed GPCP precipitation and 850hpa winds against CEN domain averaged GPCP precipitation for early and late summer, respectively. During early summer (JJ) (Fig. 4.11a), the regression pattern reveals that the precipitation is east-northwest aligned, where as during late summer (AS) (Fig. 4.11b), the precipitation is west-central aligned, and we can also notice CEN precipitation negatively associated with northeast India precipitation in the late summer months (AS). Figure 4.11c shows the regression map of large-scale convergence and moisture transport for

early summer (JJ). Strong convergence from the head Bay of Bengal sector is associated with the precipitation variability over CEN region and the large scale cyclonic circulation is basically from the Bay of Bengal sector in the early summer (Fig. 4.11a, c). During late monsoon season (AS), the large-scale cyclonic circulation over the northwest and central parts of India enveloping peninsular India is strongly associated with precipitation variability over CEN region. Active convergence over Arabian Sea and cyclonic moisture circulation favour positive precipitation anomalies over central India (Fig. 4.11b, d). A similar picture evolves in the ERA-40 dataset (Figure not shown) for early and late summers and also in NCEP/NCAR reanalysis in both summers (Figure not shown).

Regressed pattern of evaporation reveals a significant but weak association of evaporation over south of central India both in the early summer and in the late summer, the role of evaporation in modulating the central India precipitation anomalies is weak during late summer compared to early summer (Fig. 4.11e, f). Thus, we can say that both (ΔC) and (ΔE) plays a role in the interannual variability of (P) over central India during early (JJ) and late summer (AS) months.

GPCP precipitation and 850hpa winds regressed with NEI domain averaged GPCP precipitation for early summer (JJ) is shown in Fig. 4.12a and for late summer (AS) is shown in Fig. 4.12b. During the early summer, the NEI precipitation is largely associated with NEI domain itself. Strong association over southeast of the domain and weak association with central domain are evident from the regression map. During late summer (AS), the positive association is more localized and a negative association with NWI precipitation is also seen (Fig. 4.12b). Large-scale convergence (C) and moisture transport regressed with NEI domain averaged GPCP (P) for early summer (JJ) is shown in Fig. 4.12c. We notice convergence northwest of the domain regressed positively with the precipitation index. Though regression is weak, the positive precipitation anomalies

are coupled with the cyclonic circulations from the Bay of Bengal and the upper reaches of the climatological position of monsoon trough, which is similar to the typical condition of monsoon break, where dry condition prevails over most part of the Indian subcontinent. Movement of the low level trough (monsoon trough) to foothills of the Himalayas causes break condition over the subcontinent (Raghavan 1973, Krishnamurti and Bhalme, 1976) and the northeast Indian (NEI) regions receive above normal rainfall. A typical break like circulation brings positive precipitation anomalies over northeast India (NEI) during early summer (JJ) (Fig. 4.12a, c).

During late monsoon season (AS) the cyclonic circulation is confined only over the northeast India, strong divergent flux is noticed over the south Bay of Bengal and large-scale divergent flux encompasses most part of the Indian subcontinent showing a typical dry condition over the entire subcontinent. The positive precipitation anomalies over NEI are favoured by localized convergence and moisture transport from the northern Bay of Bengal (Fig. 4.12b, d). A similar picture is evidenced in the ERA-40 results and in NCEP/NCAR reanalysis results, which suggests that precipitation over NEI domain is inversely related the rest of the domains.

Both in early summer and late summer, evaporation also plays a key role in modulating the precipitation anomalies over NEI (Fig. 4.12e, f). A similar result can be seen in ERA-40 dataset (Figure not shown) and NCEP/NCAR dataset (Figure not shown). The convergence (C) computed from these datasets may vary due to different data assimilation techniques and model orography. So, we have made interpretations based on the over all representation of (ΔE) and (ΔC) to P variability due to the presence of complex orography over this region and P at NEI is less reliable due to orography and a data sparse area.

Figure 4.13a, b shows GPCP precipitation and 850hpa winds regressed with BOB

domain averaged GPCP precipitation for early and late summer, respectively. During early summer (JJ) (Fig. 4.13a), the regression pattern reveals that the precipitation anomalies over BOB are strongly associated with (P) over head Bay of Bengal and along the Burma coast and no association with (P) over the central and south of the domain, where as during late summer (AS) (Fig. 4.13b) the precipitation anomalies have profound effect over the entire BOB domain. The precipitation during early summer (JJ) are generally caused by the excessive evaporation from the Bay of Bengal and strong divergence over the head Bay of Bengal transports moisture to the land region north of it, but strong divergence prevails over south peninsular India. Therefore, Bay of Bengal acts as a source of moisture for the monsoon trough region through excessive evaporation during early summer (Fig. 4.13a, c). During late summer (AS), the anti-cyclonic circulation subsides over Bay of Bengal sector and strong moisture transport from Arabian sea coupled with higher evaporation over Bay of Bengal sector contributes to positive precipitation anomalies over Bay of Bengal (Fig. 4.13b,d). From the regressed pattern of (E), the role evaporation is evident in both early and late summers over BOB to (P) variability (Fig. 4.13e, f).

Thus from the regression patterns of C and E, the precipitation variability especially over NEI is negatively related with other domains over the sub-continent. We can clearly notice that the processes causing anomalies over different sub-domains for early and late summer are different.

4.8. Discussions

Thus the atmospheric water balance analysis over south Asia has revealed that the early summer (JJ) and the late summer (AS) precipitation anomalies over south Asia

show different features. The interannual variability of precipitation over central India and northwest India during early and late summers represents the interannual variability of precipitation over the entire Indian subcontinent. The precipitation anomalies over northeast Indian region are inversely related to anomalies over the rest of the subcontinent during the late summer monsoon season is evident through the water budget analysis. The interannual variability of precipitation over Northwest India is influenced by large-scale moisture convergence for both early and late summers and the interannual variability of precipitation over central India is influenced by both large-scale moisture convergence and the local evaporation for both early and late summers. However, over the northeast India the surface conditions during early and late summers may also partly play a role in modulating the precipitation anomalies, since the convergence is poorly correlated with precipitation in all the reanalysis datasets and the CC between (P) and (E) are strong and moderate amount evaporation is also found over land. However, one has to keep in mind that the representation of orography over this region in the reanalysis model is relatively poor and the calculated (C) and the observed (P) may have some errors and the relative role of land surface hydrological processes can not be ruled out and further studies are required to understand the role of land surface processes in modulating the precipitation anomalies over the NEI region.

A probable interaction between land and atmosphere over the CEN, NEI domains cannot be ruled out during summer monsoon season due to the role of evaporation over these regions. Though evaporation is obtained as a residual from observed (P) and calculated (C), we believe that the evaporation obtained as a residual from the water balance can at least partly explain the land-atmospheric interaction with some limitations than evaporation obtained directly from reanalysis datasets. Recently, using ensembles of GCM models Koster et al. (2005) showed that soil moisture hot spots

(regions where precipitation is sensitive to soil moisture anomaly) exists over some relatively dry monsoon regions. The land-atmospheric interaction over the domains (CEN, NEI) is crucial in understanding the soil moisture impact on precipitation. The stronger role of evaporation (ΔE) to (ΔP) as observed during early summer over CEN and during late summer over NEI shows some surface hydrological processes responsible for precipitation anomalies over these regions. It is also consistent with the previous studies such as, Yoshimura et al. (2004) that the origin of land evaporation (around 36%) is responsible for precipitation over Calcutta region (NEI domain) during July 1998 using coloured moisture analysis. As the evaporation is very much controlled by the amount of precipitation over land and the accuracy of precipitation is also important in this method, so further studies are needed to confirm such interactions. Also, Roads and Betts (2000) have studied the surface water and energy budgets for Mississippi River basin using NCEP/NCAR and ECMWF reanalyses and highlighted the limitations of both the reanalyses and recommended that further developments are needed in the current models, if we want to study the importance of land atmospheric interaction in detail.

The atmospheric water balance analysis based on JRA-25 reanalysis dataset is reliable as the P and C correlations are highest over land domains among the reanalysis datasets. Contrastive features are evident between land and Oceanic regions. Especially the BOB domain precipitation is very much controlled by higher evaporation and so, the SST over BOB domain is crucial for controlling precipitation variability over not only BOB, in addition to the influence to majority of land domains.

Both for early and late season precipitation over BOB is significantly correlated with the south-westerlies of 850hpa wind circulation and vertically integrated moisture transport over the CEN and PEN domains. Therefore precipitation variability over BOB region very much controls the precipitation variability over rest of the land domains as

well, especially during late summer season (Figures 4.11 b, d and 4.13 b, d). The reliability of precipitation over the oceans (BOB) and the calculated convergence (C) over the oceans (BOB) are however, less reliable due to lack of sufficient observations. Caution may be needed for (P) and (C) correlation over BOB, since those from the three reanalysis data show considerably large differences (as shown in table 4.1). However, we can give high priority for JRA-25 reanalysis dataset for analysis involving water balance studies on regional scale.

4.9. Conclusions

We investigated the space-time characteristics of atmospheric water balance components over south Asia in detail using selected sub domains from available model and observed datasets and summarize our results as follows,

a) JJAS based precipitation anomalies fail to capture the interannual variations of Indian Monsoon rainfall, since the large time-space differences are noticed between early summer (JJ) and late summer (AS) anomalies.

b) The contribution of convergence and evaporation to seasonal mean precipitation over the CEN domain for early summer (JJ) and late summer (AS) are different, suggesting that the mechanism of precipitation generation during early and late summers are basically different.

The different structure of (P) variability over CEN for the early and late monsoon season implies that the modulating component of precipitation for early and late summers is not the same. The changes in large-scale convergence affect (P) variability in the late summer season compared to early season. Similarly the surface condition during early summer season very much affect the (P) variability compared to late summer over CEN domain.

c) The interannual variability of precipitation over the whole Indian subcontinent measured by AISMR is closely related mainly to the precipitation variability over northwest India and central India.

During early summer, the large-scale convergence over the Bay of Bengal sector and during late summer the large-scale convergence over Arabian Sea sector have the potential of modulating the monsoon for early and late summer, respectively, on interannual time scales.

d) The precipitation variability over northwest and central India is quite different from the north east India

It is evident from the atmospheric water balance that the processes causing anomalies over NEI is different from CEN, NWI. Therefore, the northeast India (NEI) regional monsoon variability does not contribute to the interannual variability over rest of the Indian subcontinent. There exists a strong inverse relationship between NEI domain and rest of the domains over the Indian subcontinent during late summer period.

e) On the interannual time scales, the NEI domain precipitation anomalies are not directly influenced by large-scale convergence both in early and late summers, whereas the evaporation is likely to play at least partly a role in modulating the anomalies over NEI. These results suggest that some surface hydrological processes are responsible for modulating monsoon over NEI domain during summer season. Still, this is a tentative result, as the accuracy of computed (C) and observed (P) over this region has known limitations.

Thus by dividing the summer monsoon period (JJAS) into early summer (JJ) and late summer (AS), the interannual variability of water budget components for early and late summer monsoon period have revealed different characteristics of E, P and C relationships among different sub domains.

CHAPTER 5

INTERANNUAL VARIABILITY OF ATMOSPHERIC WATER BALANCE OVER SOUTH PENINSULAR INDIA AND SRI LANKA DURING NORTHEAST MONSOON SEASON

5.1. Overview

This study focuses on the North East Monsoon Rainfall (NEMR) variability. While most parts of India receive nearly the entire portion of their annual rainfall from the South West Monsoon Rainfall (SWMR), the southeast peninsular India falls under the rain-shadow region due to the presence of Western Ghats during the summer season. This region therefore critically depends on the NEMR to supplement the inadequate precipitation during SWMR. Over the southeastern tip of the Indian peninsula and neighbouring Sri Lanka, nearly 50% of the annual rainfall is received during the NEMR season.

The impact of El Nino/Southern Oscillation (ENSO) on the SWMR has been explored intensively (Ramusson and Carpenter, 1983; Krishna Kumar et al., 1999; Chang et al., 2001; Ailikun and Yasunari, 2001; Kawamura et al., 2005). The El Nino years are generally associated with below-normal SWMR rainfall (Rasmusson and Carpenter, 1983; Yasunari, 1990), where as the El Nino years are associated with above-normal

NEMR rainfall (Suppiah, 1996, 1997). Recently Pankaj Kumar et al. (2007) studied the ENSO-NEMR relationship prior to 1976 and the later periods and concluded that the ENSO-NEMR relationship has strengthened considerably in the recent decades.

Earlier studies have pointed out that a unique ocean-atmosphere mode exists in the Indian Ocean (IO), with anomalous warm SSTs over the western IO and anomalous cold SSTs in the eastern IO (Saji et al. 1999). This mode induces an unusual rainfall distribution in the surrounding areas, and is termed as the Indian Ocean Dipole Zonal Mode (IODZM) (Hastenrath et al., 1993; Webster et al., 1999). This dipole mode modulates the Maha (September and October) rainfall over Sri Lanka (Zubair et al., 2003). Similar study on NEMR over south peninsular India (Kripalani and Kumar, 2004) had revealed that NEMR and IOD are directly related, suggesting that the positive dipole phase enhances the northeast monsoon activity and the negative dipole phase suppresses the northeast monsoon activity. In viewing the previous studies on northeast monsoon rainfall variability, only ocean-atmospheric coupling has been stressed in detail, whereas land-atmospheric interactions remain unknown, to study such a role, the atmospheric water budget can provide some lead.

To understand mechanisms other than ocean-atmospheric interaction over this region, we have tried to exploit the advantages of atmospheric water balance method over south peninsular India and Sri Lanka. A few earlier global water budget studies have shown the importance of water budget analysis (Oki et al., 1995; Trenberth and Guillemot, 1998; Trenberth, 1999). What can be gained by budget analysis? Through assessing convergence (C) and evaporation (E), we can understand the hydrometeorological aspect of precipitation (P) dynamics.

The main motivation of the present study is to understand the nature of the large-

scale water balance over south peninsular India and Sri Lanka during NEMR season (OND) and to understand the mechanism behind year-to-year precipitation variability over this region. For this purpose, the space-time characteristics of monthly and NEMR (OND) interannual variations of precipitation (P), convergence of water vapour flux (C) and evaporation (E) during the period, starting from 1979 up to 2005 has been studied in detail. A particular attention is paid to understand, where does the precipitation (P) come, i.e., from large-scale moisture convergence (C) due to atmospheric circulation, and/or from evaporation (E) from the surface since both ocean-atmosphere interactions and land-atmosphere interactions are fundamental in understanding the variability of precipitation over this region. Another aspect is how P, C and E are modified on interannual time scale by the slowly varying boundary conditions and how they are related is also explored in detail.

The structure of this chapter is as follows. Section 5.2 describes the datasets and the computational procedures used in this study. In Section 5.3, we discuss the seasonality of northeast monsoon over south peninsular India and Srilanka. In Section 5.4, we document the basic features of the monthly annual cycle of water balance components (E, P, C) and seasonal march of precipitation over the selected domain and Section 5.5 presents a discussion of the interannual variability of precipitation and atmospheric water balance components. Section 5.6 discusses NEMR index with various climatic indices. Section 5.7 discusses the teleconection of NEMR with various climate anomalies and the aspect of large-scale anomalies of atmospheric water balance for excess and deficient monsoon phases, IOD mode phases and Nino-3.4 anomaly phases. In Section 5.8, the main conclusions and discussion are addressed.

5.2. Data and Method of Analysis

The period of analysis covers NEMR monsoon season of OND from 1979 up to 2005. The data products used are Global Precipitation and Climatology Project (GPCP) Precipitation (Adler et al., 2003), VASClimO (Variability Analysis of Surface Climate Observations) land gridded precipitation dataset 1950-2000 (Beck et al., 2005). The monthly sea surface temperature for the period 1982-2005 obtained from NOAA (NOAA Optimum Interpolated SST dataset) (Reynolds et al., 2002).

Water budget calculations and data analyses were performed for the 27-yr period from January 1979 through December 2005, as the reliable precipitation data over both land and ocean are available from 1979. The total vertically integrated moisture convergence is computed for the above period from NCEP/NCAR reanalysis datasets.

The study area over the south peninsular India and Sri Lanka is shown in Fig. 5.1. During the summer monsoon season (JJA), the south peninsular region receives less rainfall compared to rest of India due to the presence of Western Ghats (Fig. 5.2a); the region is a rain shadow region for summer monsoon. Considerable amount of mean seasonal precipitation over this region is evident during NEMR season (OND) (Fig. 5.2b). The annual contribution of OND precipitation exceeds 50% over the southeast peninsular India and Sri Lanka (Fig. 5.2c).

5.3. Seasonality over Peninsular India and Sri Lanka

To clearly distinguish the season over south peninsular India and Sri Lanka, the monthly mean moisture flux vectors along 80E is shown in Fig. 5.3a and the spatial mean pattern of moisture convergence and moisture flux vectors during OND season is shown in Fig. 5.3b. We can clearly notice the reversal of moisture transport vectors from south-westerlies to northeasterlies around 10-12 N during October (Fig. 5.3a). Though the mean precipitation during SON is higher than OND, OND has been chosen as northeast

monsoon rainfall season (NEMR) by considering the wind field. The percentage contribution of annual precipitation exceeds 50% over southeastern coastal peninsular India during OND and also the moisture transport vectors becomes completely northeasterlies during OND over this region.

5.4. Monthly Annual Cycle of Atmospheric Water Budget over the Selected Domain

The monthly mean annual cycle of precipitation (P), evaporation (E) and convergence (C) over the selected domain containing both south peninsular India and Sri Lanka are shown in Fig. 5.4 a,b. Before explaining the relative contribution of (C) or (E) to precipitation (P) on monthly scale, let us briefly explain the seasonal march of precipitation over the domain.

5.4.1. Monthly evolution of Precipitation over the PEN& SL domain

To examine the monthly precipitation evolution for (PEN and SL) the domain averaged monthly mean precipitation for the period 1979-2005 is plotted in Fig. 5.4a from GPCP dataset. The monthly annual rainfall pattern has double peak namely first one at June and another one at October. The NEMR monsoon season (OND) over this region exhibits a very short rainy season and relatively low magnitude of precipitation unlike the southwest monsoon over the entire south Asian region. The precipitation amount gradually increases from March and attains a peak in the month of June and sustains the peak till July and slowly falls in the successive months, but does not fall completely and second peak pattern appear in October. This is because of the precipitation from northeast monsoon, mainly due to reversal of winds from southwesterly to northeasterly. The moisture carried from the Bay of Bengal through northeasterly winds during OND brings precipitation over the peninsular India and Sri Lanka. The northeast monsoon precipitation is especially significant over the state of Tamil Nadu (Dhar and Rakhecha,

1983; Pankaj Kumar et al., 2007). Nearly 50% of annual precipitation over this region is realized during October to December period.

5.4.2. Atmospheric water budget during NEMR Season

Rainfall over the domain (Fig. 5.4b) during NEMR months (OND) are favoured by higher evaporation throughout the season shown as the box [E]. (E) is higher than (P) during pre-monsoon months and winter. Evaporation almost equals precipitation throughout the rainy season (E ~ P) (Fig. 5.4b).

Over this region, convergence (C) becomes positive from June to November season. Convergence shows only one peak during July unlike precipitation during June and October for SW and NE monsoon months, respectively. The double peak in the convergence is not very clear (Fig. 5.4b) which may due to the prevalence of weak convergence over the peninsular India. Strong convergence is seen only over Sri Lanka and the southeastern tip of peninsular India, implies that the mean evaporation during OND over peninsular India must be stronger than Sri Lanka.

Most of the earlier studies have shown that the ocean acts as the source of moisture during the NEMR monsoon months for this domain (Zubair et al., 2003; Kripalani and Kumar 2004). Here, we have found that evaporation (E) is higher than convergence (C) in magnitude during OND and (E) contribution to precipitation (P) during OND is also significant. Thus, (E) contribution to precipitation (P) exceeds (C) contribution to (P) during OND months and the evaporation from the land surface also aid precipitation during the NEMR season.

5.5. Interannual Variation of Atmospheric Water Budget over Peninsular India and Sri Lanka

To study the precipitation variability on interannual time scale, the interannual

variations of water budget components are plotted for OND over the domain. The correlation coefficient (CC) between precipitation and moisture convergence are used to understand the relationship between P and C on the interannual time scale and similarly for the evaporation.

The contribution of evaporation to mean seasonal precipitation is high over the south peninsular India and Sri Lankan region during NEMR monsoon period and also for interannual variability, the correlation between (ΔP) and (ΔC) is 0.73 (exceeds 95% significant level) and the correlation between (ΔP) and (ΔE) is 0.84 (exceeds 95% significant level) (Fig. 5.4c). Thus, the contribution of evaporation during the monsoon months to the year-to-year variability of precipitation has been brought out through the atmospheric water budget clearly, i.e., ($\Delta E > \Delta C$). The correlation between precipitation and the residual evaporation at 0.84, suggests that the land surface hydrological processes are also important to understand the P variability on interannual timescales over this region.

One important point to be noted here is that, the correlation coefficient (CC) between (ΔP) and (ΔC) as well as (ΔP) and (ΔE) are highly significant (significant above 95% level). Thus the (P) variability over this domain during NEMR season (OND) is not only dependent on the large-scale convergence (ΔC), but also on (ΔE). Strong land-atmospheric interactions do coexist along with ocean-atmospheric interactions over this region during OND.

5.6. Averaged NEMR Monsoon Index versus IOD and NINO-3.4 Indices

To identify the significant influence of various climate anomalies to NEMR variability (dominant climate anomalies like El Nino/La Nina and IOD anomalies), the

NEMR precipitation index has been created using the observed GPCP precipitation over the selected domain and this index is used for discussing the strength of the monsoon over the south peninsular India and Sri Lanka during OND months shown in Figure 5.5 Based on the available observed GPCP rainfall data, a time series of NEMR over the south peninsular India and Sri Lanka has been developed. Similarly, an index to quantify the Indian Ocean dipole (IOD), exhibiting warm (cool) waters over the equatorial western (southeastern) Indian Ocean and Nino-3.4 anomalies has been developed using NOAA-IO optimum interpolated SST data for the period (1982-2005).

The NEMR, IOD (Difference of SST between western Indian Ocean (WIO) (10S-10N, 55E-70E) and southeast Indian Ocean (SEIO) (10S-0N, 90E-120E) and NINO-3.4 (5S-5N, 190E-240E) SST anomalies are standardised with their respective standard deviations and plotted. We have considered October to December (OND) season to represent the NEMR, whereas the IOD, El Nino and La Nina phases are represented by September to November (SON) season, since the IOD peaks in the months of SON. Saji and Yamagata (2003) have shown that the largest combined contribution of ENSO and IOD to the zonal and meridional wind variability over the Indian Ocean is during SON around 45% between 10S and 10N. The correlation coefficient between NEMR and IOD is found to be less significant (0.24), whereas the correlation coefficient between NEMR and NINO-3.4 anomalies are significant (0.46) at 95% significant level, which is also evident from the recent studies that the impact of ENSO on NEMR is strengthening in the recent decades (Pankaj Kumar et al., 2007). The excess/deficient NEMR, IOD and NINO3.4 positive/negative phase are obtained by applying a criterion that the standardised anomalies exceed +/- 0.5 standard deviation (SD).

5. 7. Teleconnections and Large-Scale Anomalies of (P) and (C) and (E) between Anomalous Monsoon Years, ENSO and Indian Ocean Dipole Mode Years

In this section, we discuss the various teleconnections of NEMR and the differences in atmospheric circulation for anomalous NEMR monsoon years and IOD positive-negative phase years over the selected domain.

To show the teleconnection patterns of NEMR, the NOAA-OI optimum interpolated global SST (1982-2005) for OND is regressed with the selected domain's OND GPCP precipitation (Fig. 5.6b). A significant positive correlation (significant at 95%) over the Nino-3.4 regions and over Bay of Bengal near Myanmar coast and South China Sea, a less significant negative correlation over the Southeast Indian Ocean over the coast of Sumatra are noticed and no correlations are observed with IOD.

The regressed pattern of precipitation reveals a significant negative relationship with the Indo-China peninsula precipitation during NEMR monsoon (OND) season (Fig. 5.6a). Figure 5.6c shows that the convergence over the Indian Ocean is significantly associated with the domain precipitation and the moisture flux vectors largely originate from the Southeast Indian Ocean region. Figure 5.6d shows that evaporation also plays an active role in modulating the interannual variability of NEMR precipitation over the PEN and SL domain.

In Figs. 5.7 and 5.8, anomalies of precipitation (P), large-scale convergence (C), moisture transport vectors and evaporation (E) are plotted for anomalous NEMR monsoon years, IOD positive-negative phase years and also Nino-3.4 anomaly phase years in order to understand the physical mechanism or dynamics through which of (P) variability over the domain occur.

The excess or deficient years are obtained by applying the criterion that the standardised anomalies exceed +/- 0.5 SD. Similarly the IOD and NINO3.4 phases are

also selected by applying the same criterion.

5 excess years, 8 deficient years, 5 IOD positive phases, 7 IOD negative phase, 8 El Nino phases and 8 La Nina phases were selected from (1982-2005) 24 years dataset for analysis as shown in Table (1). The excess and deficient years composite anomaly from the seasonal mean climatology are plotted to understand the difference between different phases and their mechanism.

The dynamics of the NEMR - IOD relationship are examined using the P, C and E by constructing standardised anomaly composite patterns for each phase. The excess precipitation composite anomaly pattern (Fig. 5.7a) caused by enhanced convergence and enhanced moisture transport from the southeast Indian Ocean and the south Bay of Bengal towards south peninsular India and Sri Lanka are shown in Fig. 5.7d. The evaporation composite anomaly is also positive during excess years (Fig. 5.7g). The precipitation anomaly in Fig. 5.7a is similar to the positive IOD phase composite anomaly pattern (Fig. 5.7b) and also similar to the El-Nina composite anomaly pattern (Fig. 5.7c). Similarly, the convergence composite anomalies (Fig. 5.7d) over the equatorial Indian Ocean resembles IOD phase (Fig. 5.7e) as well as El Nino Phase (Fig. 5.7f) except a slight higher divergence over the Bay of Bengal region in both IOD and El Nino phases. Evaporation anomaly over the domain is slightly positive during the excess years (Fig. 5.7g) compared to IOD positive phase (Fig. 5.7h) and El Nino phase (Fig. 5.7i). Thus the overall features of excess NEMR seems to be influenced by the combined effect of IOD positive and El Nino phases. So, we can say that positive NEMR is approximately equal to the effects of positive IOD phase and El Nino phase.

Standardised composite anomaly for deficient NEMR, IOD negative and La Nina phases are shown in Fig. 5.8. The deficient NEMR precipitation composite anomaly

pattern (Fig. 5.8a) shows very strong deficient precipitation, associated with strong divergence and enhanced anti-cyclonic moisture transport over the Arabian Sea and south peninsular India and Sri Lanka and the adjacent Oceanic regions (Fig. 5.8d). The evaporation composite anomaly is also negative during the deficient years (Fig. 5.8g). The precipitation anomaly over the domain during deficient years (Fig. 5.8a) is not similar to the negative IOD phase composite precipitation anomaly pattern (Fig. 5.8b), but has some similarity to the La Nina composite precipitation anomaly pattern (Fig. 5.8c), the precipitation anomaly during deficient years are quite strong compared to La Nina composite precipitation anomaly pattern. The IOD negative phase induces precipitation anomaly over the equatorial India Ocean, but has a little impact on the south peninsular India and Sri Lanka, as we can notice positive precipitation anomaly over south peninsular India and adjacent region during IOD negative phase (Fig. 5.8b). Similarly, the convergence composite anomaly for negative IOD phase (Fig. 5.8e) is confined over the equatorial Indian Ocean, convergence over southeastern Indian Ocean and the Bay of Bengal and divergence over the western equatorial Indian Ocean, which does not resemble the deficient composite anomaly phase (Fig. 5.8d) as well as La Nina Phase (Fig. 5.8f). The composite convergence anomaly pattern during the deficient phase (Fig. 5.8d) and La Nina anomaly pattern (Fig. 5.8f) are quite similar. And also the evaporation composite anomaly for deficient years (Fig. 5.8g) is similar to La Nina anomaly years (Fig. 5.8i) and does not compare with negative IOD years (Fig. 5.8h). Thus, the overall features of deficient NEMR seems to be influenced only by La Nina phase. So, we can say that negative NEMR is approximately equal to the effects of La Nina phase.

The asymmetrical influence of IOD mode on NEMR is also evident in the

composite anomaly maps of SST. Figure 5.9a, b, c shows the SST composite anomaly for NEMR excess years, IOD positive phase and El Nino phase, respectively. The pattern more or less agrees with one another except the IOD phase anomaly composite, which shows enhanced east-west dipole mode (Fig. 5.9b). Both in excess NEMR and El Nino phases the East-west dipole is subdued (lower magnitude of anomalies on either side). So, we can say that the excess NEMR monsoon is favoured by colder SST anomalies over the southeast tropical Indian Ocean and warmer SST anomalies over tropical western Indian Ocean (a typical IOD positive phase) associated with El Nino conditions over tropical Pacific Ocean. Moreover, the SST anomalies over the Bay of Bengal are also important as this basin is responsible for generating tropical cyclones, which significantly affects the precipitation over NEMR domain during OND (Pankaj Kumar et al., 2007).

In contrast, Fig. 5.10 a, b, c shows the SST composite anomaly for NEMR deficient years, IOD negative phase and La Nina phase, respectively. In the deficient composite years the SST pattern over the southeast tropical Indian Ocean exhibits a warmer SST anomaly and colder anomaly over the western tropical Indian Ocean (Fig. 5.10a), but we can notice a large pool of negative anomaly over Bay of Bengal, which is absent in the IOD negative Phase (Fig. 5.10b). The negative anomaly over the Bay of Bengal basin is not favourable for the formation of tropical cyclones, which in turn affects the precipitation over the NEMR domain considerably. The SST composite patterns resemble the La Nina phase quite well (Fig. 5.10c), though the pool of SST anomaly is confined to the eastern part of the Bay of Bengal basin. In the IOD negative phase SST composite pattern (Figure 5.10b), only the east-west SST difference is enhanced but quite different from the La Nina and NEMR deficient years composite

patterns.

Therefore, the precipitation (P), sea surface temperature (SST), convergence (C), evaporation (E) and moisture circulation anomalies associated with the positive IOD and excess NEMR are consistent where as the precipitation (P), sea surface temperature (SST), convergence (C), evaporation (E) and moisture circulation anomalies associated the negative IOD and deficient NEMR are inconsistent. This result suggests the asymmetrical influence of IOD mode on the NEMR during OND rainfall over south peninsular India and Sri Lanka is evident. Moreover, ENSO has (basically) symmetrical influence, but IOD has not. IOD influence is confined only to positive NEMR.

Apart from the ocean-atmospheric interactions, we also notice some land-atmosphere interactions. Recently, by using ensembles of GCM models Koster et al. (2005) showed that soil moisture hot spots exist over some relatively dry monsoon regions. The land-atmosphere interactions over these domains are crucial in understanding the soil moisture impact on precipitation. They have shown that over the transition zones between wet and dry climates, soil moisture anomalies are translated into precipitation anomalies. In dry climates, evaporation rates are sensitive to soil moisture but are also generally small and small evaporation rates should have a limited ability to affect precipitation. Only in the transition zones between wet and dry climates, the atmosphere is conducive for precipitation generation where evaporation is suitably high due to sufficient soil moisture, so we can expect soil moisture to influence precipitation. The excess evaporation during entire season (OND) as observed in Fig. 5.3b may support such a hypothesis based on GCM results. We can notice significant and strong regression coefficient of evaporation also over land apart from adjacent oceanic regions in the domain (large-scale residual evaporation regressed with the domain precipitation) (Fig.

5.6d). But the validity of such hypothesized processes needs much more detailed study. Thus, the positive (+NEMR) case is favoured by both evaporation from land surface and enhanced evaporation from positive SST (+SST) over the Bay of Bengal (BOB), while during negative (-NEMR), large-scale downward motion due to La Nina inhibits higher evaporation over land and adjacent Oceans.

5.8. Conclusions and Discussion

We investigated the interannual variability of atmospheric water balance components over south peninsular India and Sri Lanka during NEMR (OND) season and summarize our results as follows,

(1) Asymmetrical influence of Indian Ocean Dipole mode on the northeast monsoon rainfall anomaly during OND over the south peninsular India and Sri Lanka.

The precipitation (P), sea surface temperature (SST), convergence (C), evaporation (E) and moisture circulation anomalies associated the positive IOD and excess NEMR years are similar each other where as the precipitation (P), sea surface temperature (SST), convergence (C), evaporation (E) and moisture circulation anomalies associated with negative IOD and deficient NEMR years are not similar to each other. This result suggests that the influence of IOD mode on the NEMR is not symmetrical, whereas an asymmetrical influence of IOD mode on the NEMR is evident.

(2) Apart from strong ocean-atmospheric interactions, some land-atmospheric interactions do coexist over this domain.

The contribution of evaporation (E) is higher for seasonal mean precipitation (P) over the domain, and the interannual variability of precipitation (ΔP) is determined not only by evaporation (ΔE), but also by the large-scale convergence (ΔC).

The interannual variability of precipitation over the south peninsular India and Sri Lanka is influenced by both evaporation over land and adjacent oceans and the large-scale moisture convergence from the south Indian Ocean region is evident from the water budget analysis. However, the large-scale circulation anomalies can modulate the evaporation over the domain and subsequently modulate precipitation. Mainly, the evaporation over the adjacent oceanic regions acts as the source of moisture for precipitation, but the evaporation over the land is also considerably high. The land surface processes over the domain during NEMR monsoon season may also play a role in modulating the precipitation anomalies. However one has to keep in mind that the grid resolution of the model (reanalysis) is relatively poor and the calculated (C) and observed (P) may have errors, but still the relative role of land surface hydrological processes can not be ruled out and further studies are required to understand the role of land surface processes in modulating the precipitation anomalies over this region during NEMR (OND) season. The major findings of this study are also briefly summarized in Table (2).

Therefore, we discuss that the Land, the Atmosphere and the Ocean interactively modulate the NEMR over the south peninsular India and Srilanka during OND. So far, the existence of the hot spots of land atmosphere interactions of significant coupling strength in relatively dry monsoon regions during summer monsoon (JJAS) season are known from ensemble of GCM studies (e.g. Koster et al. 2005). From our study, we have found that the land surface processes may also contribute to precipitation anomalies over south peninsular India and Sri Lanka during (OND) northeast monsoon season.

CHAPTER 6

CONCLUSIONS

In this Chapter, the results from the studies are summarized and future scope of studies are also discussed,

C.1. Summary

1. The space-time characteristics of atmospheric water balance revealed that over the south Asia, the mechanism of precipitation generation for early and late summers are different over most of the domains.
2. The year-to-year variability of summer precipitation over most of the domain is determined by large-scale convergence except over the NEI domain.
3. A probable role of surface hydrological process in modulating the precipitation variability over NEI cannot be ruled out. Role of such surface hydrological processes needs to be studied further.
4. The notable result from the atmospheric water balance over peninsular India and Sri Lanka during October to December revealed the asymmetrical influence of IOD on northeast monsoon rainfall (NEMR).
5. Another interesting result brought out over peninsular India is the probable role of land-atmosphere interaction in modulating precipitation variability during OND.

C.2. Discussion

Thus the interannual variability of both vital monsoon systems over south Asia has been explored using atmosphere water balance method. The mechanism of precipitation evolution for the early summer (JJ) and the late summer (AS) over south Asia has shown different features. Early summer (JJ) being influenced by systems from

the Bay of Bengal and late summer (AS) from the Arabian Sea sector, and the role of evaporation and convergence during both the seasons of summer were also dealt in detail. The interannual variability of precipitation over central India and northwest India during early and late summers represents the interannual variability of precipitation over the entire Indian subcontinent or AISMR. The precipitation anomalies over northeast Indian region are independent of anomalies over the rest of the subcontinent during the late summer monsoon season has been clearly shown. Over the northeast India the surface conditions during early and late summers may also play a role in modulating the precipitation anomalies (similar results are obtained in most of the reanalysis), needs further studies to ascertain it as a fact.

An asymmetrical influence of Indian Ocean Dipole mode on the northeast monsoon rainfall anomaly during OND over the south peninsular India and Sri Lanka as been brought out clearly by atmospheric water budget analysis. Most of the earlier studies brought out only strong ocean-atmosphere coupling over south peninsular India and Sri Lanka. With the help of atmospheric water budget analysis we have shown the active role of land-atmosphere interactions on interannual time scales and concluded that over the south peninsular India and Sri Lanka during OND, the land, the atmosphere and the ocean interactively modulate NEMR.

C.3. Discussion connecting JJAS and OND

Some similarities and some differences are noted between the south west monsoon domains and northeast monsoon domain (south peninsular India).

Over the south peninsular India during southwest monsoon and northeast monsoon seasons, the mean evaporation exceeds moisture convergence, which is similar to the dry regions of northwest India. Similarly over central India, the mean evaporation

becomes higher during late summer (AS). These similarities suggest that the evaporation contribution to seasonal mean precipitation over the Indian subcontinent is reasonably high.

On the interannual time scales, the (ΔE) contribution to P variability is significant over peninsular India during northeast monsoon season. Similarly, the (ΔE) contribution to P variability is significant over northwest India during southwest monsoon season. However, a difference has been noted between central India and peninsular India. The (ΔE) contribution to P variability is not significant during late summer (AS) over central India; this could be due to the active moisture convergence over the central India from the Arabian Sea sector. Thus, the region where seasonal mean evaporation is high and interannual variability of P is dependent on (ΔE) is vulnerable to droughts.

C. 4. Future Scope of Study

Further dynamical downscaling using regional climate model can be carried out to obtain high resolution dataset to study in detail the atmospheric water budget over south Asia.

Water resources play a vital role in every sector over south Asia and the fact that the hydrological cycle is a fundamental component of climate makes it imperative that adequate attention needs to be paid to the regional water resources. It is desirable to study water budget for major river basins like Ganges, Godavari and Krishna applying water balance method using fine spatial resolution precipitation dataset.

It is also desirable to undertake extensive regional modeling to understand the characteristics of land atmospheric interaction on precipitation variability over the south Asian Monsoon region.

Appendix

HIGH RESOLUTION ATMOSPHERIC WATER BALANCE ANALYSIS OVER SOUTH ASIAN DOMAIN

In this Appendix we show the characteristic features of atmospheric water balance over south Asia using high-resolution reanalysis datasets (JRA-25 reanalysis, VASClimO). The analysis here basically focuses to reassure whether the similar features get reflected during early, late summer seasons and during post monsoon season as noted in the previous chapters 4 and 5. The JRA-25 reanalysis has a resolution of 1.25°x1.25°. Computed convergence (C) from high-resolution dataset provides an opportunity to study in detail, the local variability of P, C and E. In this chapter, evaporation is obtained as a residual from VASClimO (P) and JRA-25 (C). We discuss briefly the mean seasonal features of P, C and E and interannual correlations of P with (C) and (E).

A.1. Seasonal mean precipitation, convergence and evaporation over south Asia

The seasonal mean amount of precipitation (P), evaporation (E) and convergence (C) over south Asia are shown in Fig. A.1. During, the early summer season (JJ), precipitation is large over west coast and northeast India (Fig. A.1a). As evidenced in the low-resolution model results during early summer, the convergence is mainly dominant over the Bay of Bengal sector and the convergence is aligned east and northwest (Fig. A.1b). The mean evaporation is high over the west coast and over the northeast India (Fig. A.1c).

Similarly, during the late summer season (AS) (Fig. A.2a), the precipitation is large over west coast and the Bay of Bengal and moderate precipitation over central India too. During the late summer, the convergence becomes stronger over the central India (Fig. A.2b). The evaporation is high over the west coast and over the northeast India and considerable evaporation over central India also is noticed (Fig A.2c).

During the NEMR season (OND) (Fig. A.3a), the precipitation is moderate over the east coastal region and southeast peninsular India. Precipitation is large over Sri Lankan region. During NEMR season, the convergence is weaker over the entire Indian region (Fig. A.3b), but the evaporation is high over the south east coast of India (peninsular India) and over the northeast India and over central India considerable evaporation is noticed (Fig A.3c).

A.2. Interannual variation of atmospheric water budget over south Asia

To understand the dynamics of (P) variability on interannual timescales, correlation between (P) & (C) and (P) & (E) are computed on grid scale. We can notice significant correlations of (P) and (C) over central India (Fig. A.1d). Moreover, significant correlations of (P) and (E) are noticed over northeast India and over west coast (Fig. A.1e), suggesting some surface hydrological processes in modulating the (P) variability over these regions. The residual evaporation (E) obtained through water balance is sensitive to precipitation data as well as computed (C); so the residual evaporation suffers from significant errors, but still the role of surface hydrological processes cannot be ruled out completely as we could see it in most of these reanalyses results.

A significant relationship between (P) and (C) over central India in the late summer is also evident (Fig. A.2d). Correlation between (P) and (E) is also significant

over patches of northeast India and west coastal regions in the late summer season (AS) (Fig. A.2e). Though, the significant (P) and (E) relationship on interannual time scale has been brought out in all the three reanalysis datasets over northeast India. Still further studies are needed to confirm these results, as the residual evaporation obtained through water balance suffers from considerable errors.

To study the precipitation variability on interannual time scale for OND. The correlation coefficient (CC) between (P) & (C) and (P) & (E) are used. Strong correlation between (P) & (E) is seen over the south peninsular India (significant at above 95% significant level) over most of the grid points (Fig. A.3e). Suggesting land surface hydrological processes are also important for (P) variability during OND over south peninsular India.

To get confidence on the reliability of calculated high resolution convergence dataset, we have made the correlations between the calculated (C) of JRA and NCEP, JRA and ERA for early and late summer; the correlations between JRA and NCEP, JRA and ERA are generally significant over most of the land points. Similarly, for OND correlation over land is significant. Thus, most of the datasets agree with each other. Only, they do not agree among them are over oceans. The reason may be due to poor observations over oceans and the data gets filled with synthetic data generated by models (using the first guess). The datasets agree among each other over regions, where high densities of observational datasets are available.

Generally, all the models agree over south Asian domain, with subtle differences among reanalyses due to differences in model and assimilated datasets. Still, atmospheric water budget is a robust method to study hydrological cycle and its variability.

REFERENCES

Adler, R.F., G.J. Huffman, A. Chang, R. Ferraro, P. Xie, J. Janowiak, B. Rudolf, U. Schneider, S. Curtis, D. Bolvin, A. Gruber, J. Susskind, P. Arkin, and E. Nelkin, 2003: The Version 2 Global Precipitation Climatology Project (GPCP) monthly precipitation analysis (1979-Present). *J. Hydrometeor.*, **4**, 1147-1167.

Ailikun, B. and T. Yasunari, 2001: ENSO and Asian summer monsoon: persistence and transitivity in the seasonal march. *J. Meteor. Soc. Japan*, **79**, 145-159.

Beck, C., J. Grieser and B. Rudolf, 2005: A new monthly precipitation climatology for the global land areas for the period 1951 to 2000. *Climate Status Report* 2004, 181 – 190.

Cadet, D. and G. Reverdin, 1981: Monsoon over the Indian Ocean during summer 1975, Part-I. *Mon. Wea. Rev*., **109**, 148-158.

Cadet, D. L. and S. Greco, 1987: Water vapour transport over the Indian Ocean during the 1979 summer monsoon. Part I: Water vapour fluxes, *Mon.Wea.Rev.*, **115**, 653-663.

Chang, C.P., P. Harr and J. Ju, 2001: Possible roles of Atlantic circulations on the weakening Indian monsoon rainfall-ENSO relationship. *J. Climate*, **14**, 2376-2380.

Dhar, O. N. and P. R. Rakhecha, 1983: Forecasting northeast monsoon rainfall over Tamil Nadu, India. *Mon. Wea. Rev*., **111**: 109-112.

Findlater, F. J., 1969: A major low level air current near the Indian Ocean during the northern summer. *Quart. J. R. Meteorol. Soc.,* **95**, 362-380.

Fukutomi, Y., H. Igarashi, K. Masuda and T. Yasunari, 2003: Interannual variability of summer water balance components in three major river basins of northern Eurasia. *J. Hydrometeorol.*, **4**, 283 - 296.

Graversen R.G, E. Kallen, M. Tjernstrom, and H. Kornich, 2007: Atmospheric mass-

transport inconsistencies in the ERA-40 reanalysis. *Quart. J. R. Meteorol. Soc.,* **133**(624): 673-680.

Goswami, B. N., D. Sengupta, and G. Suresh Kumar, 1998: Intraseasonal oscillations and interannual variability of surface winds over the Indian monsoon region, *Proc. Indian Academy of Sciences - Earth and Planetary Sciences*, **107**, 45-64.

Hastenrath, S., A. Nicklis and L. Greischar, 1993: Atmospheric hydrospheric mechanisms of climate anomalies in the western equatorial Indian Ocean. *J. Geophys. Res.*, **98**, 20,219-20,235.

Joseph, P.V. and S. Sijikumar, 2004: Intraseasonal variability of the low-level jet stream of the Asian summer monsoon, *J. Climate*, **17**, 1449-1458.

Kalnay E., Coauthors, 1996**:** The NCEP/NCAR 40-Year Reanalysis Project. *Bull. Amer. Meteor. Soc.*, **77**, 437- 471.

Kane, R. P., 1998: Extremes of the ENSO phenomenon and Indian summer monsoon rainfall. *Int. J. Climatol.,* **18**, 775-791.

Kawamura, R., K. Uemura and R. Suppiah, 2005: On the recent change of the Indian summer monsoon-ENSO Relationship. *SOLA*, **1**, 201-204.

Koster, R.D. and GLACE Team, 2004: Regions of strong coupling between soil moisture and precipitation. *Science,* **305**, 1138-40.

Kripalani, R. H., A. Kulkarni, S. S. Sabade, J. V. Revadekar, S. K. Patwardhan, and J. R. Kulkarni, 2004: Intraseasonal oscillations during monsoon 2002 and 2003, Current science, **87**(3), 325-331.

Kripalani, R. H., P. Kumar, 2004: Northeast monsoon rainfall variability over south peninsular India vis-a-vis the Indian Ocean dipole mode. *Int. J. Climatol.,* **24**, 1267-1282.

Krishnamurti, T. N. and P. Ardanuy, 1980: The 10-20 day westward propagation mode

and breaks in the monsoons, *Tellus*, **32**, 15-26.

Krishnamurti, T. N. and H. N. Bhalme, 1976: Oscillations of a monsoon system. Part I. Observational aspects. *J. Atmos. Sci.*, **33**, 1937-1954.

Krishnamurti, T. N. and D. Subrahmanium, 1982, The 30-50 day mode at 850 mb during MONEX, *J. Atmos. Sci.*, **39**, 2088-2095.

Krishna Kumar, K., B. Rajagopalan and M. A. Cane, 1999: On the weakening relationship between the Indian monsoon and ENSO. *Science*, **284,** 2156–2159.

Maity, R. and D. Nagesh Kumar 2006: Hydroclimatic association of the monthly summer monsoon rainfall over India with large-scale atmospheric circulations from tropical Pacific Ocean and the Indian Ocean region. *Atmos. Sci. Lett.,* **7**, 101-107.

Marengo J. A., 2005: Characteristics and spatio-temporal variability of the Amazon River Basin water budget. *Clim. Dyn.,* **24**(1), 11-22.

Oki T., K. Musiake, H. Matsuyama and K. Masuda, 1995: Global atmospheric water balance and runoff from large river basins. *Hydrol. Processes*, **9**, 655–678.

Onogi, K., H. Koide, M. Sakamoto, S. Kobayashi, J. Tsutsui, H. Hatsushika, T. Matsumoto, N. Yamazaki, H. Kamahori, K. Takahashi, K. Kato, T. Ose, S. Kadokura and K. Wada 2005: JRA-25; Japanese 25-year Reanalysis progress and status. Quart. J. R. Meteorol. Soc., 131, 3259-3268.

Pant G.B. and K. Rupa Kumar, 1997: Climates of South Asia. *John Wiley & Sons*, Chichester, 320pp.

Pankaj Kumar., K. Rupa Kumar, M. Rajeevan, A. K. Sahai, 2007: On the recent strengthening of the relationship between ENSO and northeast monsoon rainfall over South Asia. *Clim. Dyn.,* (2007) **28**, 649-660.

Parthasarathy, B., N. A. Sontakke, A. A. Munot, and D. R. Kothawale1987:

Droughts/floods in the summer monsoon rainfall season over different meteorological subdivisions of India for the period 1871-1984. *J. Climatol.,* **7**, 57-70.

Parthasarathy, B., K. Rupa Kumar, and A. A. Munot, 1993: Homogeneous Indian monsoon rainfall: Variability and prediction. *Proc. Indian Acad. Sci. (Earth Planet. Sci.),* 121-155.

Parthasarathy B., A. A. Munot and D. R. Kothawale, 1995: Monthly and seasonal rainfall series for all-India homogeneous regions and meteorological subdivisions:1871-1994. *Research Report No. RR-**065***, Indian Institute of Tropical Meteorology, Pune, 113pp.

Parthasarathy, B., K. Rupa Kumar, and A. A. Munot, 1996: Homogeneous regional summer monsoon rainfall over India: Interannual variability and teleconnections. IITM-Res. Report, RR-70.

Peixoto J. P. and A. H. Oort, 1992: Physics of Climate. *Amer. Inst. Phys*., 520 pp.

Raghavan, K., 1973: Break Monsoon over India, *Mon. Wea. Rev*., **101**, 33-43.

Rasmusson, E. M. and T. H. Carpenter, 1983: The relationship between eastern equatorial Pacific sea surface temperatures and rainfall over India and Sri Lanka, *Mon. Wea. Rev*., **111**, 517-528.

Reynolds, R.W., N.A. Rayner, T.M. Smith, D.C. Stokes, and W. Wang, 2002: An improved in situ and satellite SST analysis for climate. J. Climate, **15**, 1609-1625.

Roads, J.O. and A. Betts, 2000: NCEP-NCAR & ECMWF Reanalysis surface water and energy budgets for the Mississippi River Basin. *J. Hydrometeorol.,* **1** (1) 88-94.

Saha, K. R. and S. N. Bavadekar, 1973: Water vapour budget and precipitation over the Arabian Sea during the northern summer. *Quart. J. R. Meteorol. Soc.*, **99**, 273-278.

Saji N. H., B. N. Goswami, P. N. Vinayachandran, and T. Yamagata, 1999: A dipole mode in the tropical Indian Ocean. *Nature,* **401**, 360-363.

Saji, N. H. and T. Yamagata, 2003: Possible impacts of Indian Ocean dipole mode events

on global climate. *Climate Research,* **25**, 151-169.

Sikka, D. R. and S. Gadgil, 1980: On maximum cloud zone and ITCZ over Indian longitude during the southwest monsoon. *Mon. Wea. Rev*., **108**, 1840-1853.

Singh, N. and N. A. Sontakke, 1999: On the variability and prediction of post-monsoon season rainfall over India. *Int J Climatol.,* **19**, 309-339.

Suppiah R., 1989: Relationship between the southern oscillation and the rainfall of Sri Lanka. *Int. J. Climatol.,* **9**, 601- 618.

Suppiah R., 1996: Spatial and temporal variations in the relationship between southern oscillation phenomenon and the rainfall of Sri Lanka. *Int J Climatol.,* **16**, 1391-1407.

Suppiah R., 1997: Extremes of southern oscillation phenomenon and the rainfall of Sri Lanka. *Int. J. Climatol.,* **17**, 87-101.

Trenberth K. E., 1991: Climate diagnostics from global analyses: Conservation of mass in ECMWF analyses. *J. Climate*, **4**, 707–722.

Trenberth, K. E. and C. J. Guillemot, 1998: Evaluation of the atmospheric moisture and hydrological cycle in the NCEP/NCAR reanalyses. *Climate Dyn.*, **14**, 213-231.

Trenberth, K. E., 1999: Atmospheric moisture recycling: Role of advection and local evaporation. *J. Climate*, **12**, 1368-1381.

Trenberth, K. E., J. Fasullo, and L. Smith, 2005: Trends and variability in column-integrated water vapor. *Clim. Dyn.,* **24,** 741-758.

Uppala, S.M., and collaborators, 2005: The ERA-40 re-analysis. *Quart. J. R. Meteorol. Soc*., **131**, 2961-3012, doi: 10.1256/qj.04.176

Webster, P. J., Magana, V. O., Palmer, T. N., Shukla, J., Tomas, R. A., Yanai, M. and Yasunari, T, 1998: Processes, predictability and prospects for prediction. *J. Geophys. Res.*, **103**(C7), 14,451-14,510.

Webster, P. J., A. M. Moore, J. P. Loschnigg, R. R. Leben, 1999: Coupled ocean-

atmosphere dynamics in the Indian Ocean during 1997-98. *Nature,* **401**, 356-360.

Yasunari, T., 1979: Cloudiness fluctuations associated with the northern hemisphere summer monsoon. *J. Meteor. Soc. Japan*, **57**, 227-242.

Yasunari, T., 1980: A Quasi-stationary appearance of 30 to 40 day period in the cloudiness fluctuations during the summer monsoon over India. *J. Meteor. Soc. Japan*, 58, 225-229.

Yasunari, T., 1981: Structure of an Indian summer monsoon system with around 40-day period. *J. Meteor. Soc. Japan*, 59, 336-354.

Yasunari, T., 1990: Impact of Indian monsoon on the coupled atmosphere/ocean systems in the tropical Pacific. *Meteor. & Atmos. Phys*., **44**, 29-41.

Yoshimura, K., T. Oki, N. Ohte, and S. Kanae., 2004: Colored moisture analysis estimates of variations in 1998 Asian monsoon water sources. *J. Meteor. Soc. Japan*, **82**, 1315-1329.

Zubair L, S. A. Rao, and T. Yamagata., 2003: Modulation of Sri Lankan Maha rainfall by the Indian Ocean dipole. *Geophys. Res. Lett.,* **30**(2): **35**-1-**35**-4.

ACKNOWLEDGEMENTS

I deem it a distinct pleasure to acknowledge my indebtedness to all the people who have guided me to complete my thesis work. I owe a deep sense of gratitude and sincere thanks to my guide Prof. Dr. Tetsuzo Yasunari for his constant supervision, personal interest, critical evaluation and inspiring guidance in shaping this work. I would like to thank Ministry of Education, Culture, Sports, Science and Technology, Government of Japan for providing me support through Monbukagakusho scholarship. I would like to thank Dean of HyARC for giving me an opportunity to carry out my research work at HyARC, Nagoya University. I am thankful to all my student colleagues who helped me during the time of depressions, which helped me in successful completion of my thesis work. I am grateful to Dr H. Fujinami and Dr M. Hori for critically evaluating my research paper before submission. I would also like to express my thanks to Profs. Kenji Nakamura and Hiroshi Uyeda for their helpful comments and critical evaluation of my thesis. Last but not the least; I would like to acknowledge all the centers for providing datasets for free of cost.

FIGURES

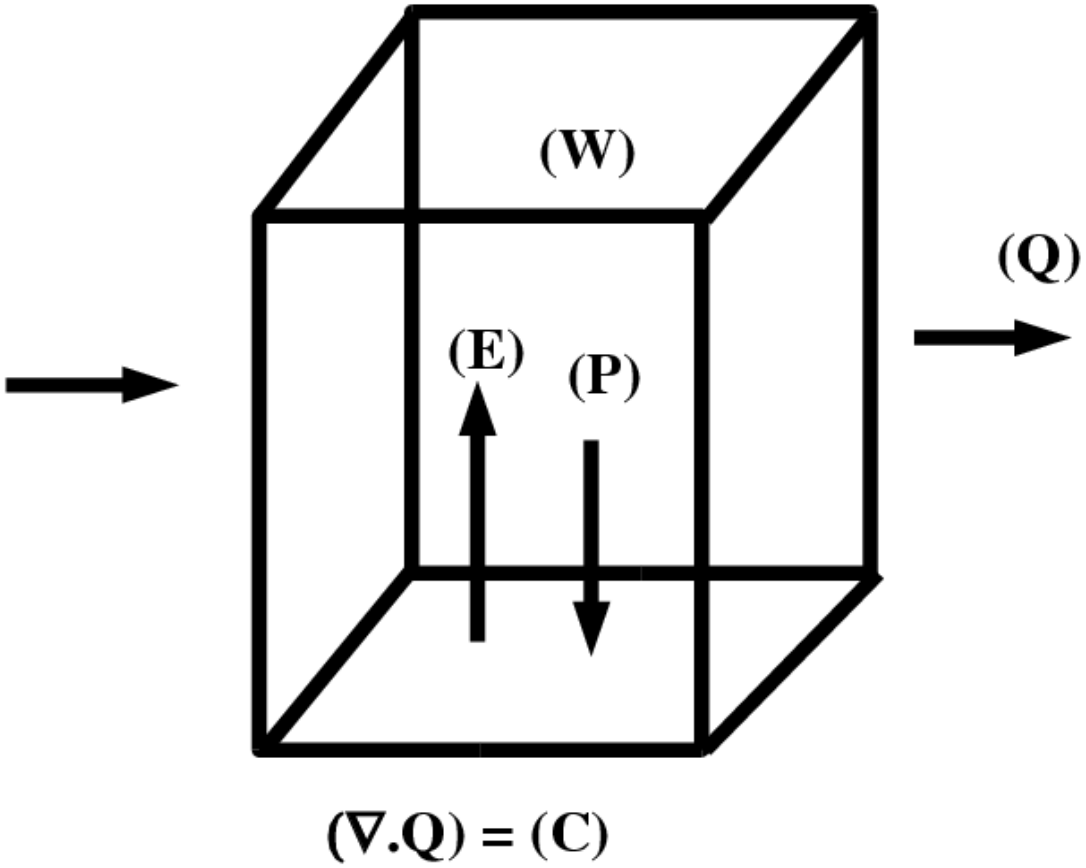

Figure 3.1. A simple Schematic diagram showing water balance over a small area on a longer time scale, where P is the precipitation, Q is the vertically integrated moisture flux. E is the evaporation from surface; W is the precipitable water content.

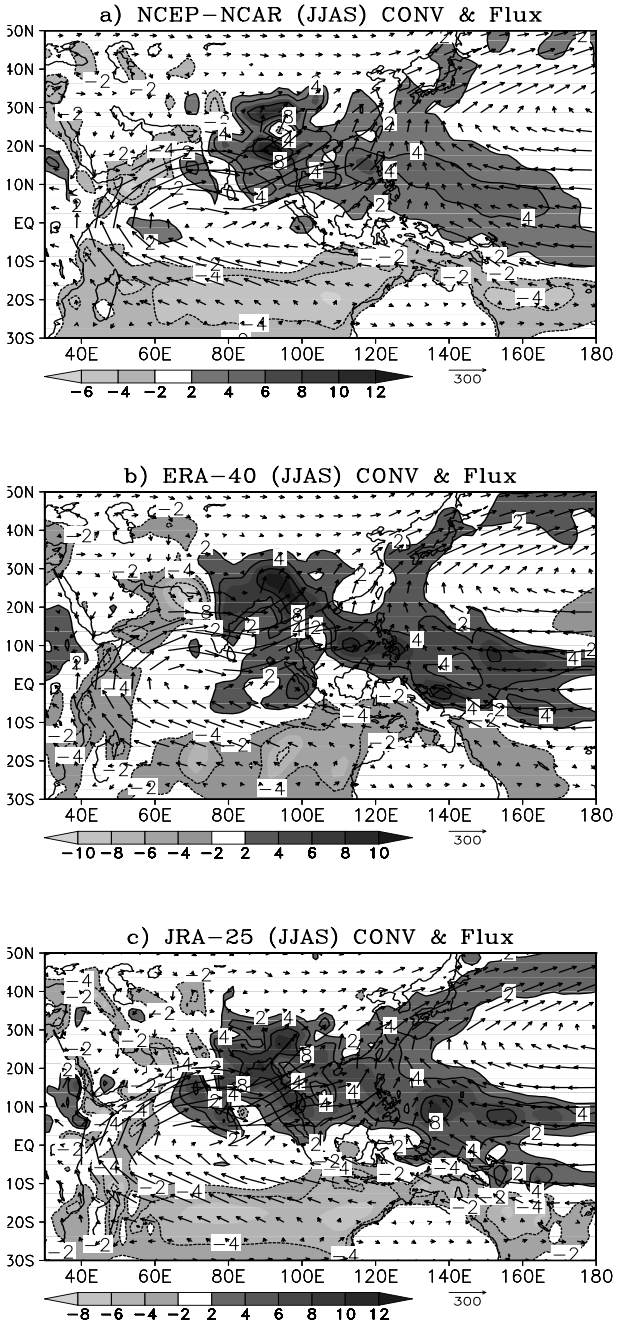

Figure 3.2. Climatological JJAS mean Convergence and moisture flux for the period 1979-2000. a) NCEP/NCAR , b) ERA-40 c) JRA-25. (Unit for convergence: mm/day and moisture flux: kg/m/s)

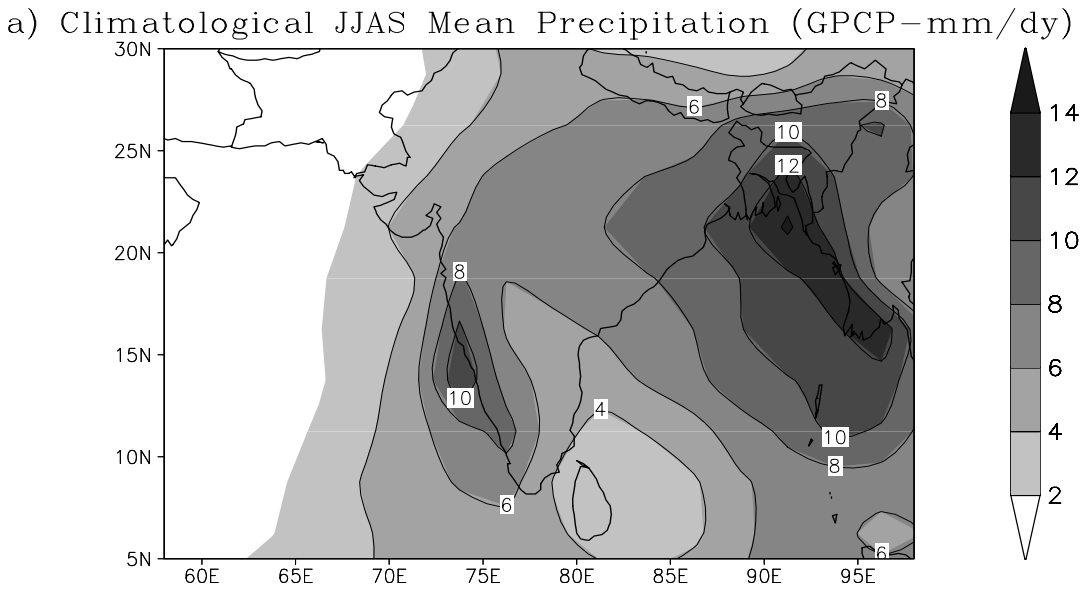

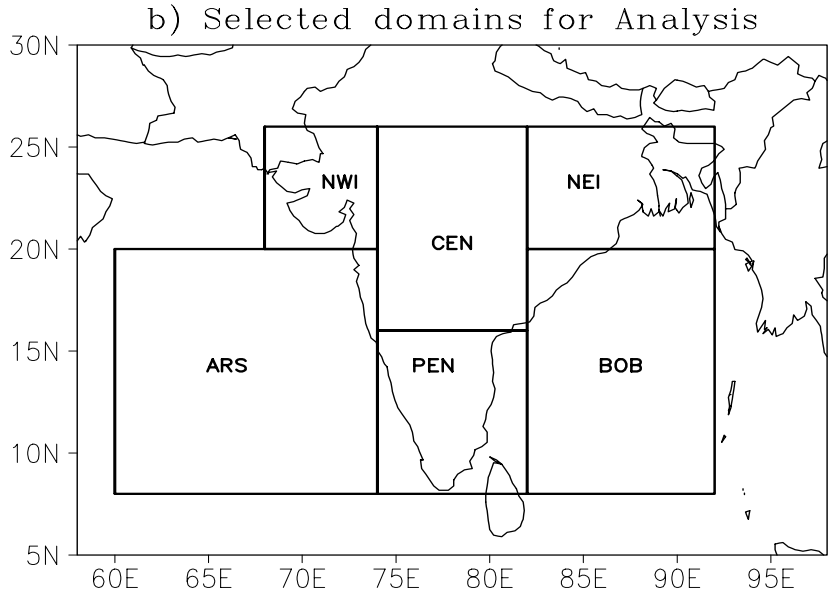

Figure 4.1. a) Climatological JJAS mean precipitation from GPCP (mm/day) for the period 1979-2000. b) Selected boxes over South Asia for analysis of atmospheric water balance. (NWI: North West India) (NEI: North East India) (CEN: Central India) (PEN: Peninsular India) (ARS: Arabian Sea) (BOB: Bay of Bengal)

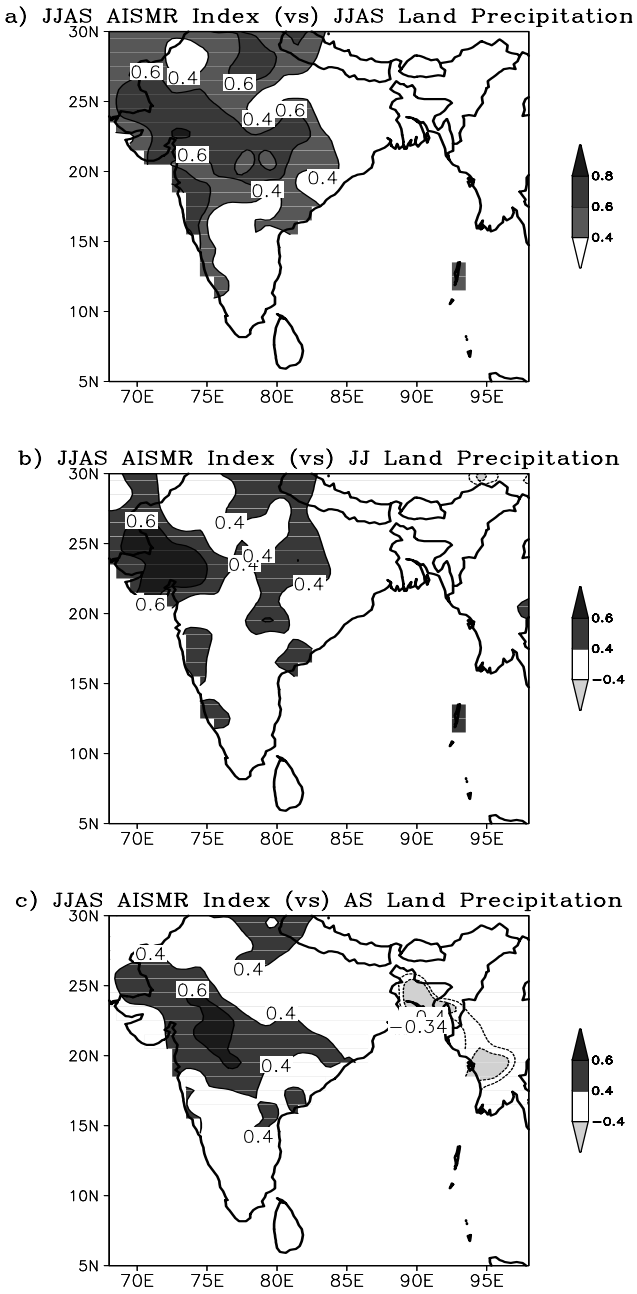

Figure 4.2. Correlation between AISMR index (JJAS) and land gridded precipitation (VASClimO) for the period 1979-2000. a) AISMR (vs.) JJAS precipitation b) AISMR (vs.) early summer precipitation (JJ) c) AISMR (vs.) late summer precipitation (AS). (Shaded values are significant at 95% level) (Shaded bar indicates correlation coefficient).

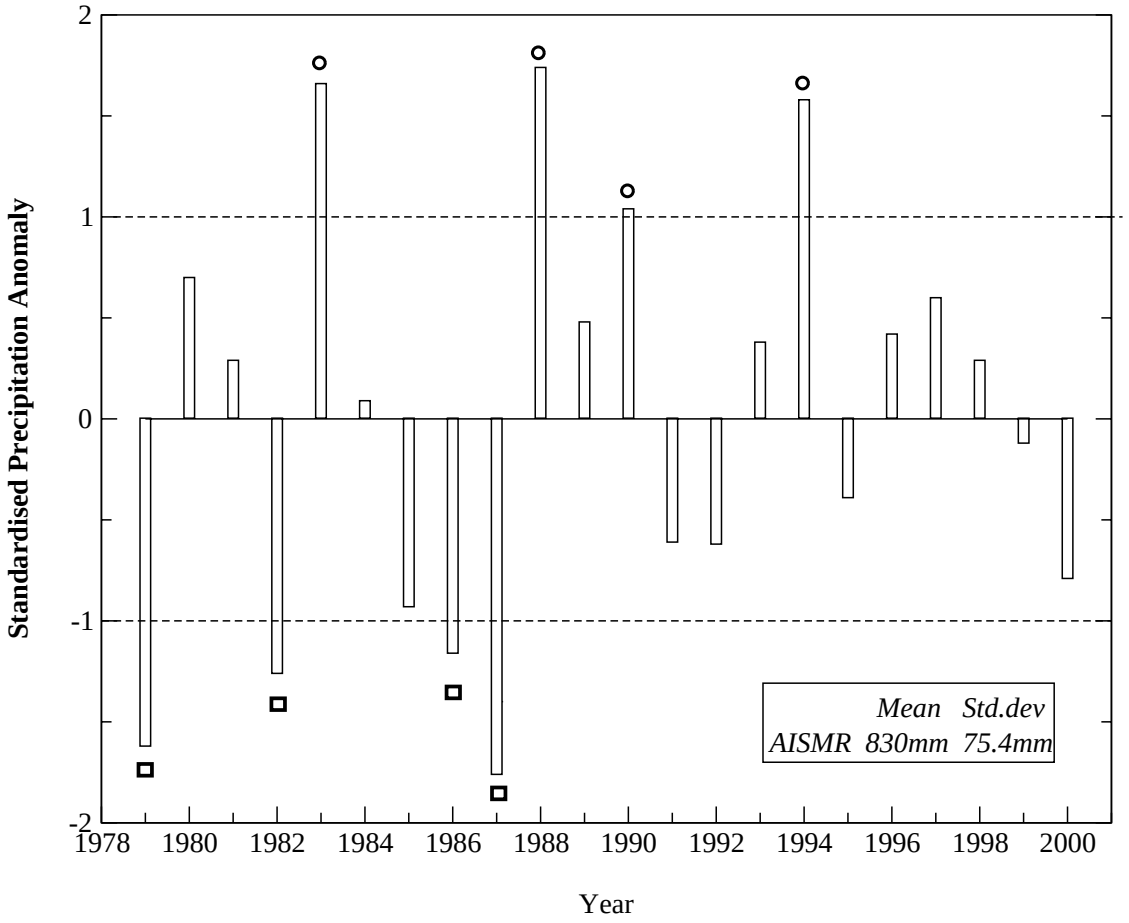

Figure 4.3. All India Summer Monsoon Rainfall (AISMR) from 1979-2000. (JJAS precipitation mean and standard deviations are given inside the box. Filled circles denote wet years and filled squares denote dry years). [Wet years: 1983,1988,1990,1994], [Dry years: 1979,1982,1986,1987]

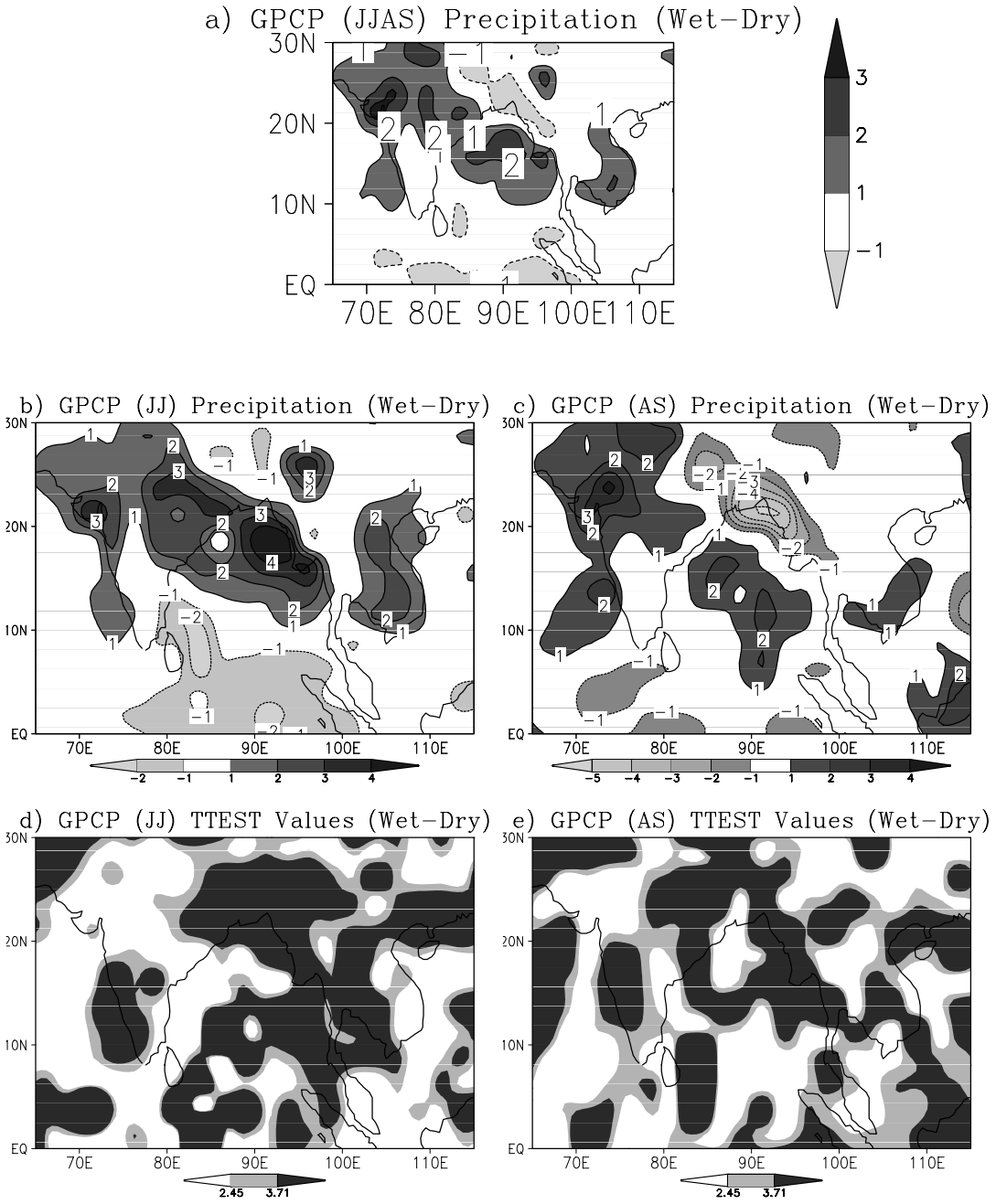

Figure 4.4. Difference between Wet and Dry years [First panel] for entire summer (JJAS), a) GPCP Precipitation. [Second Panel] b) GPCP Precipitation for early summer (JJ), c) GPCP Precipitation for late summer (AS). [Third Panel] d) t-test for GPCP precipitation (JJ), e) t-test for GPCP precipitation (AS). (Units for precipitation: mm/day, t-test values above 3.71 (99%level) and t-test values above 2.48 (95% level).

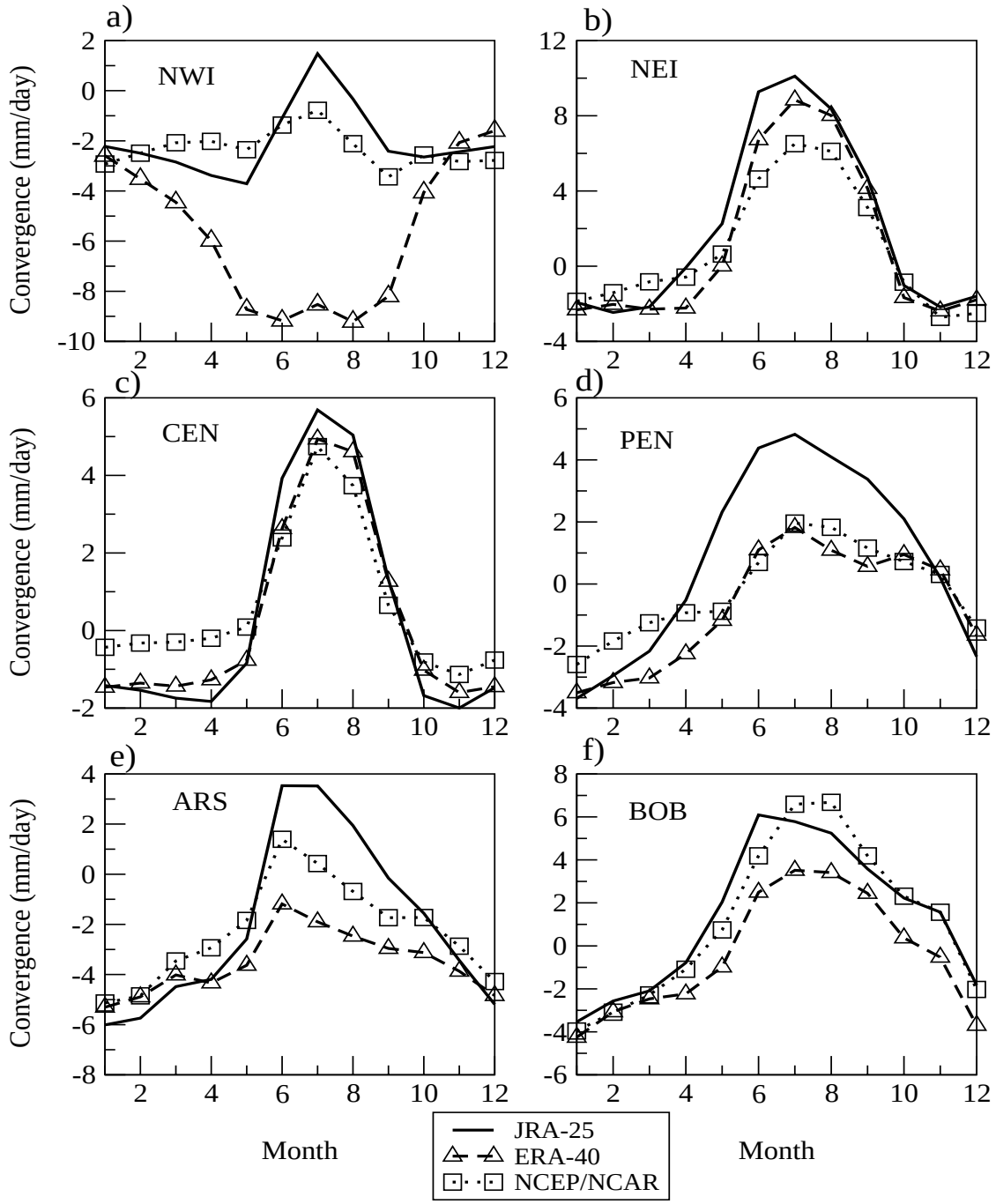

Figure 4.5. Observed monthly mean cycle of convergence (C) over different domains of South Asia in three major reanalysis (JRA-25, ERA-40 and NCEP/NCAR) datasets. (NWI: North West India) (NEI: North East India) (CEN: Central India) (PEN: Peninsular India) (ARS: Arabian Sea) (BOB: Bay of Bengal).

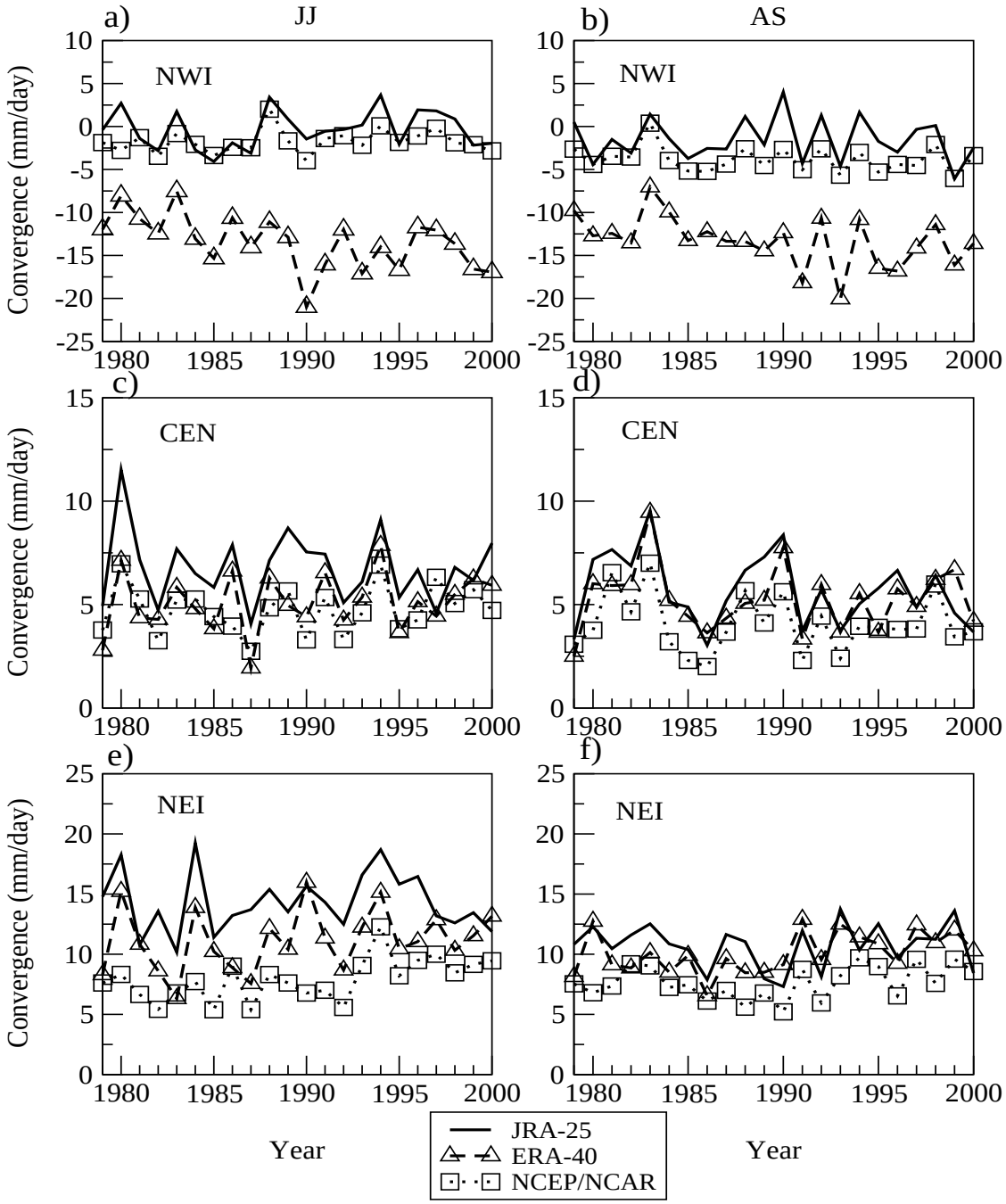

Figure 4.6. Interannual variations convergence (C) over different domains of South Asia in three major reanalysis (JRA-25, ERA-40 and NCEP/NCAR) datasets. [Top Panel] for NWI domain a) early summer (JJ) and b) late summer (AS), [Middle Panel] for CEN domain c) early summer (JJ) and d) late summer (AS). [Bottom Panel] for NEI domain e) early summer (JJ) and f) late summer (AS).

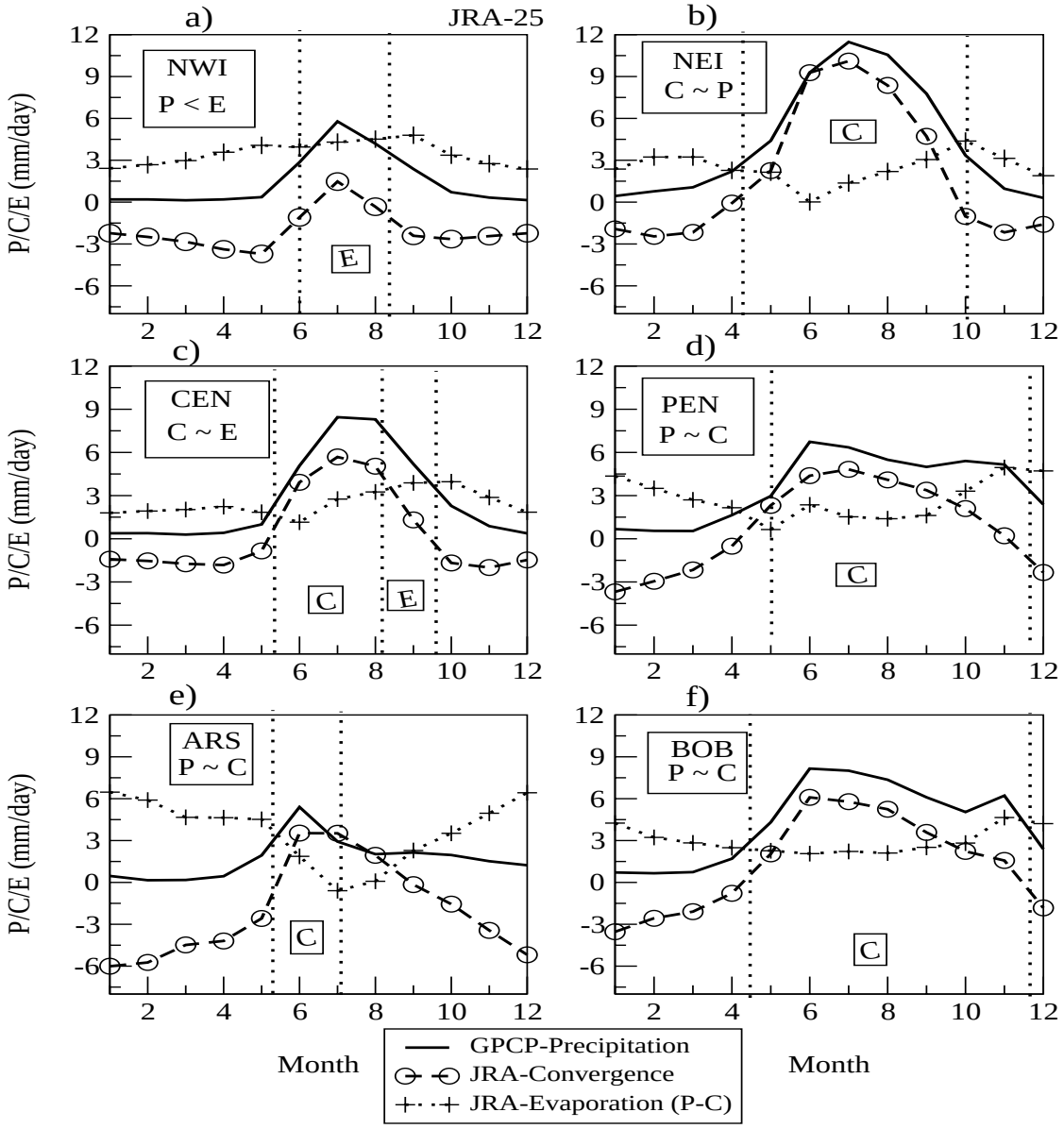

Figure 4.7. Observed monthly mean annual cycle of P, C and E over South Asia using JRA-25 dataset. (NWI: North West India) (NEI: North East India) (CEN: Central India) (PEN: Peninsular India) (ARS: Arabian Sea) (BOB: Bay of Bengal). (Dominance of convergence or evaporation is shown as C or E in boxes). Vertical dotted lines delineate the summer months from the rest of the months where dominance of E or C is valid. Box in the left top shows the relationship among P, C, and E during the monsoon season over the respective domains.

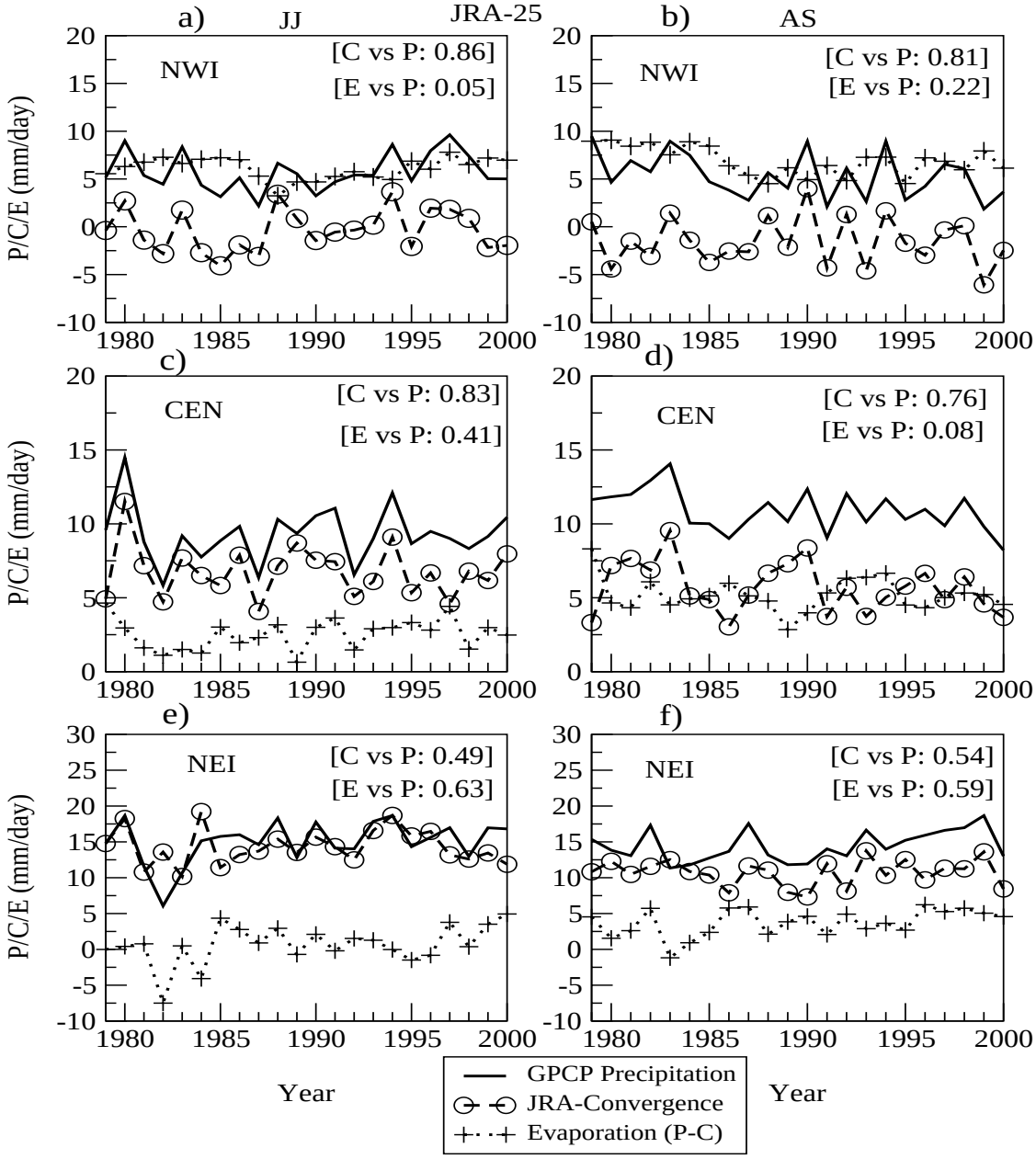

Figure 4.8. Interannual variations of P, C and E over south Asia from JRA-25 dataset. [Top Panel] for NWI domain a) early summer (JJ) and b) late summer (AS), [Middle Panel] for CEN domain c) early summer (JJ) and d) late summer (AS). [Bottom Panel] for NEI domain e) early summer (JJ) and f) late summer (AS). (Value of correlation coefficient between P and C & P and E are shown in each graph) [95% significant level is +/- 0.42]

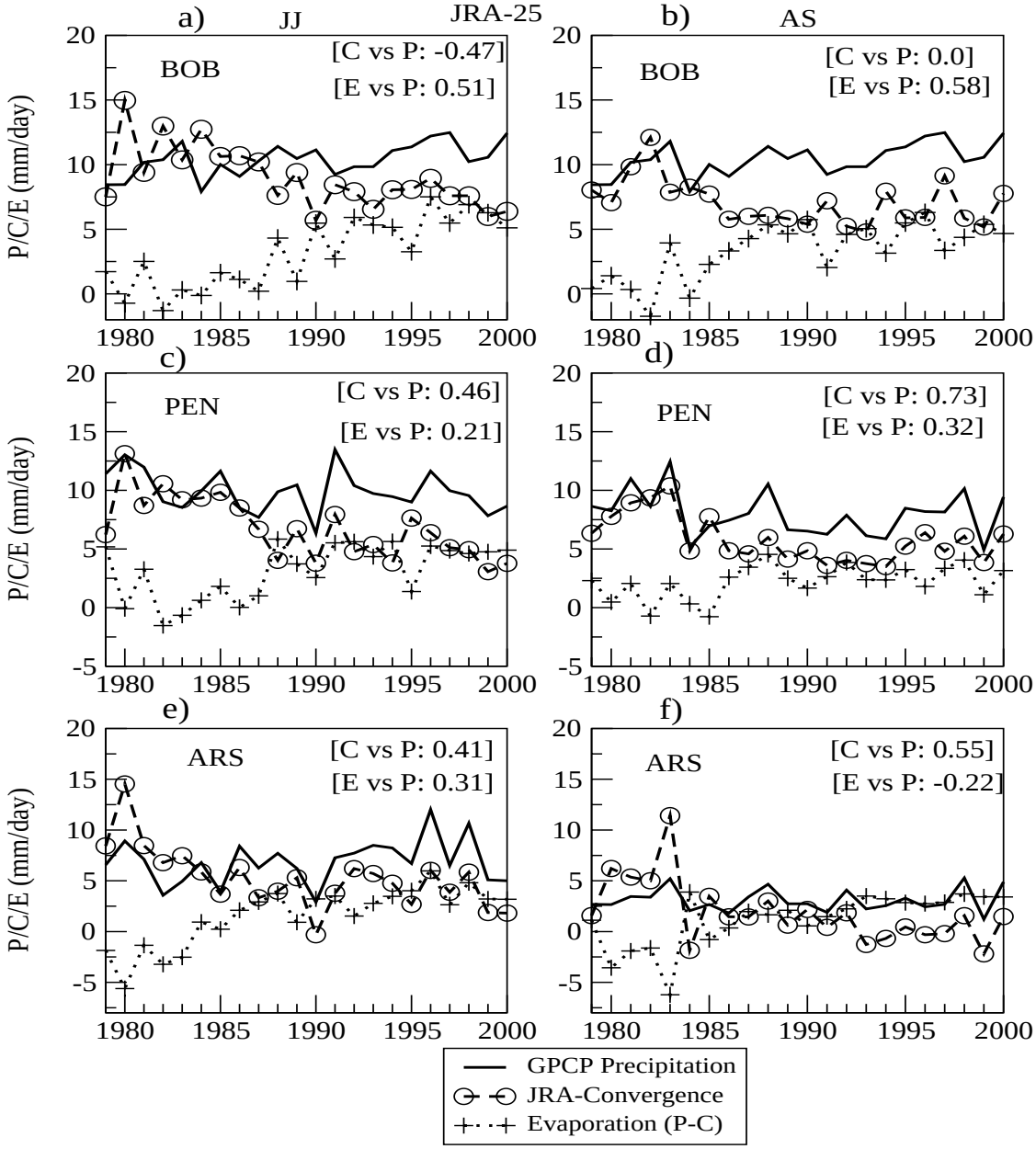

Figure 4.9. Interannual variations of P, C and E over south Asia from JRA-25 dataset. [Top Panel] for BOB domain a) early summer (JJ) and b) late summer (AS), [Middle Panel] for PEN domain c) early summer (JJ) and d) late summer (AS). [Bottom Panel] for ARS domain e) early summer (JJ) and f) late summer (AS). (Value of correlation coefficient between P and C & P and E are shown in each graph) [95% significant level is +/- 0.42]

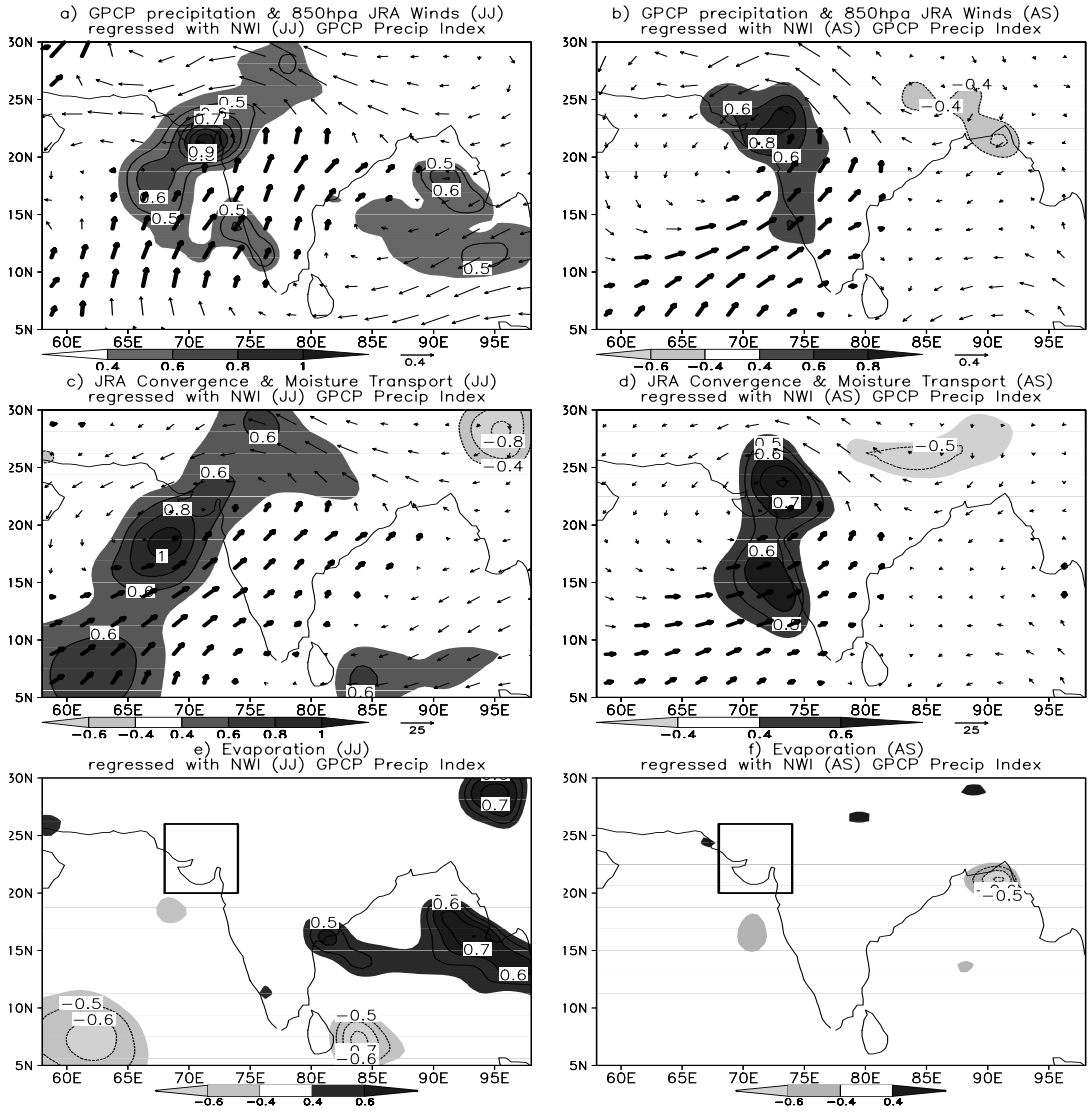

Figure 4.10. Regression maps based on Northwest India (NWI) domain averaged GPCP precipitation for JRA-25 dataset. [Top panel] GPCP Precipitation and 850hpa winds, a) for early summer (JJ) b) for late summer. [Middle Panel] Moisture Convergence and moisture flux transport, c) for early summer d) for late summer. [Bottom Panel] Evaporation, e) for early summer f) for late summer. [Domain for precipitation index is shown by a box in the Bottom panel. Shaded values and thick arrows are significant at 95% level]. (Shaded bar indicates regression coefficient), (Units for precipitation & convergence: mm/day, winds: m/sec, moisture flux: kg m^{-1} s^{-1}).

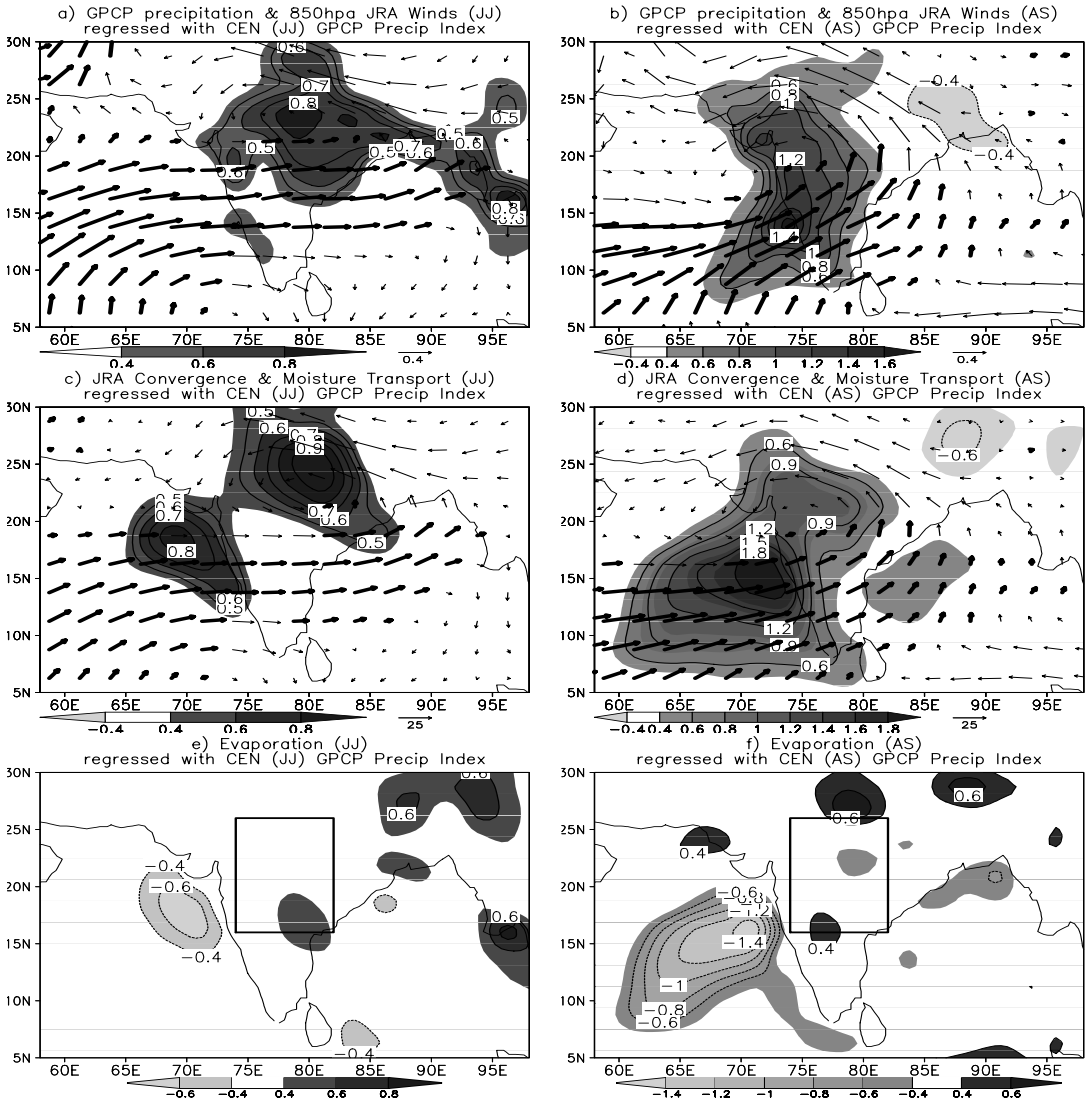

Figure 4.11. Regression maps based on Central India (CEN) domain averaged GPCP precipitation for JRA-25 dataset. [Top panel] GPCP Precipitation and 850hpa winds, a) for early summer (JJ) b) for late summer. [Middle Panel] Moisture Convergence and moisture flux transport, c) for early summer d) for late summer. [Bottom Panel] Evaporation, e) for early summer f) for late summer. [Domain for precipitation index is shown by a box in the Bottom panel. Shaded values and thick arrows are significant at 95% level]. (Shaded bar indicates regression coefficient), (Units for precipitation & convergence: mm/day, winds: m/sec, moisture flux: kg m^{-1} s^{-1}).

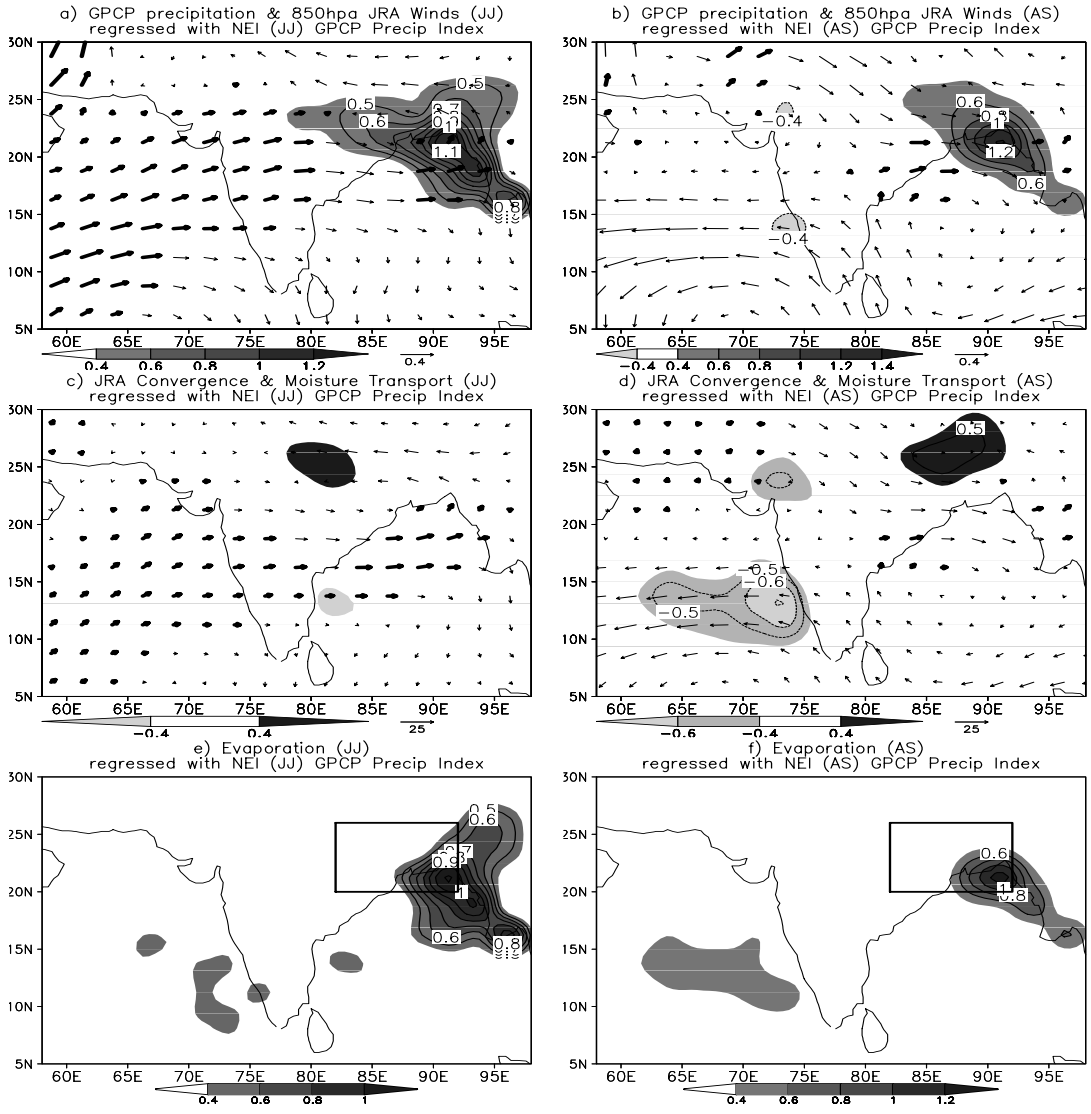

Figure 4.12. Regression maps based on Northeast India (NEI) domain averaged GPCP precipitation for JRA-25 dataset. [Top panel] GPCP Precipitation and 850hpa winds, a) for early summer (JJ) b) for late summer. [Middle Panel] Moisture Convergence and moisture flux transport, c) for early summer d) for late summer. [Bottom Panel] Evaporation, e) for early summer f) for late summer. [Domain for precipitation index is shown by a box in the Bottom panel. Shaded values and thick arrows are significant at 95% level]. (Shaded bar indicates regression coefficient), (Units for precipitation & convergence: mm/day, winds: m/sec, moisture flux: kg m^{-1} s^{-1}).

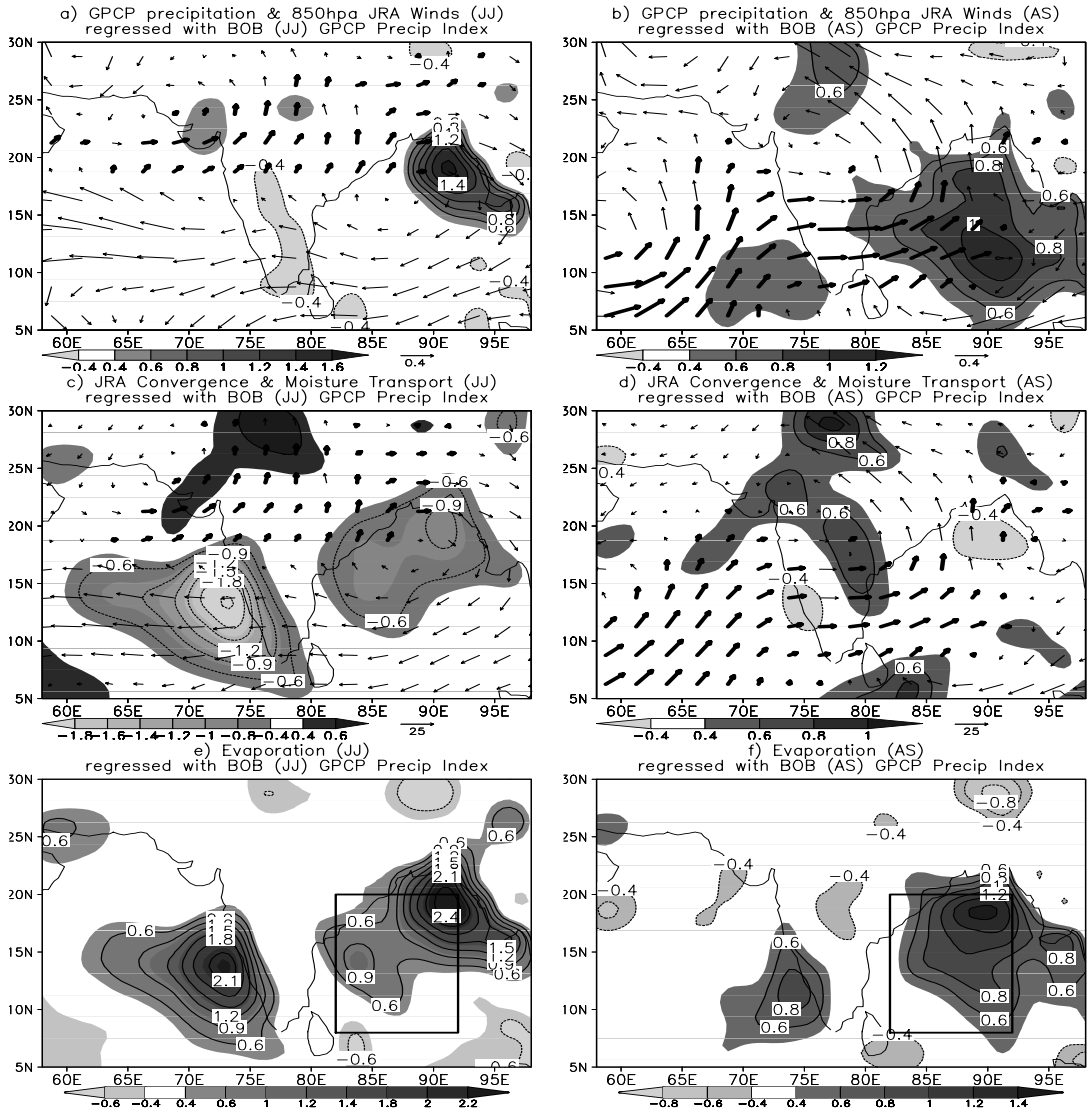

Figure 4.13. Regression maps based on Bay of Bengal (BOB) domain averaged GPCP precipitation for JRA-25 dataset. [Top panel] GPCP Precipitation and 850hpa winds, a) for early summer (JJ) b) for late summer. [Middle Panel] Moisture Convergence and moisture flux transport, c) for early summer d) for late summer. [Bottom Panel] Evaporation, e) for early summer f) for late summer. [Domain for precipitation index is shown by a box in the Bottom panel. Shaded values and thick arrows are significant at 95% level]. (Shaded bar indicates regression coefficient), (Units for precipitation & convergence: mm/day, winds: m/sec, moisture flux: kg m^{-1} s^{-1}).

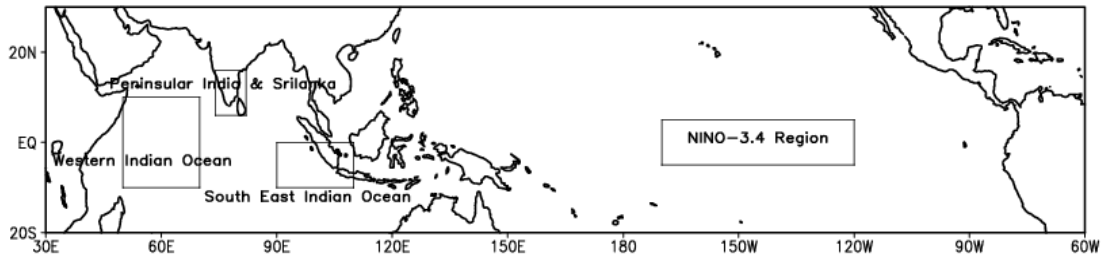

Figure 5.1. Maps showing selected domains for analysis in this study.

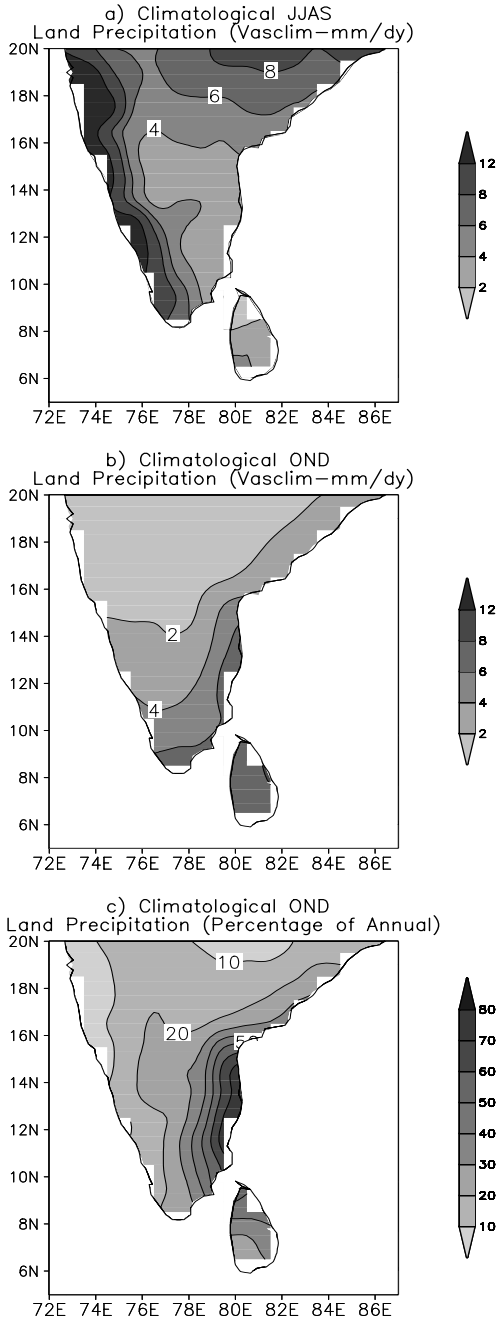

Figure 5.2. Climatological mean precipitation from VASClimO surface land observation dataset for the period 1979-2000. a) JJAS mean precipitation (mm/day) b) Climatological mean OND precipitation (mm/day) c) Percentage of OND precipitation contribution to annual mean precipitation.

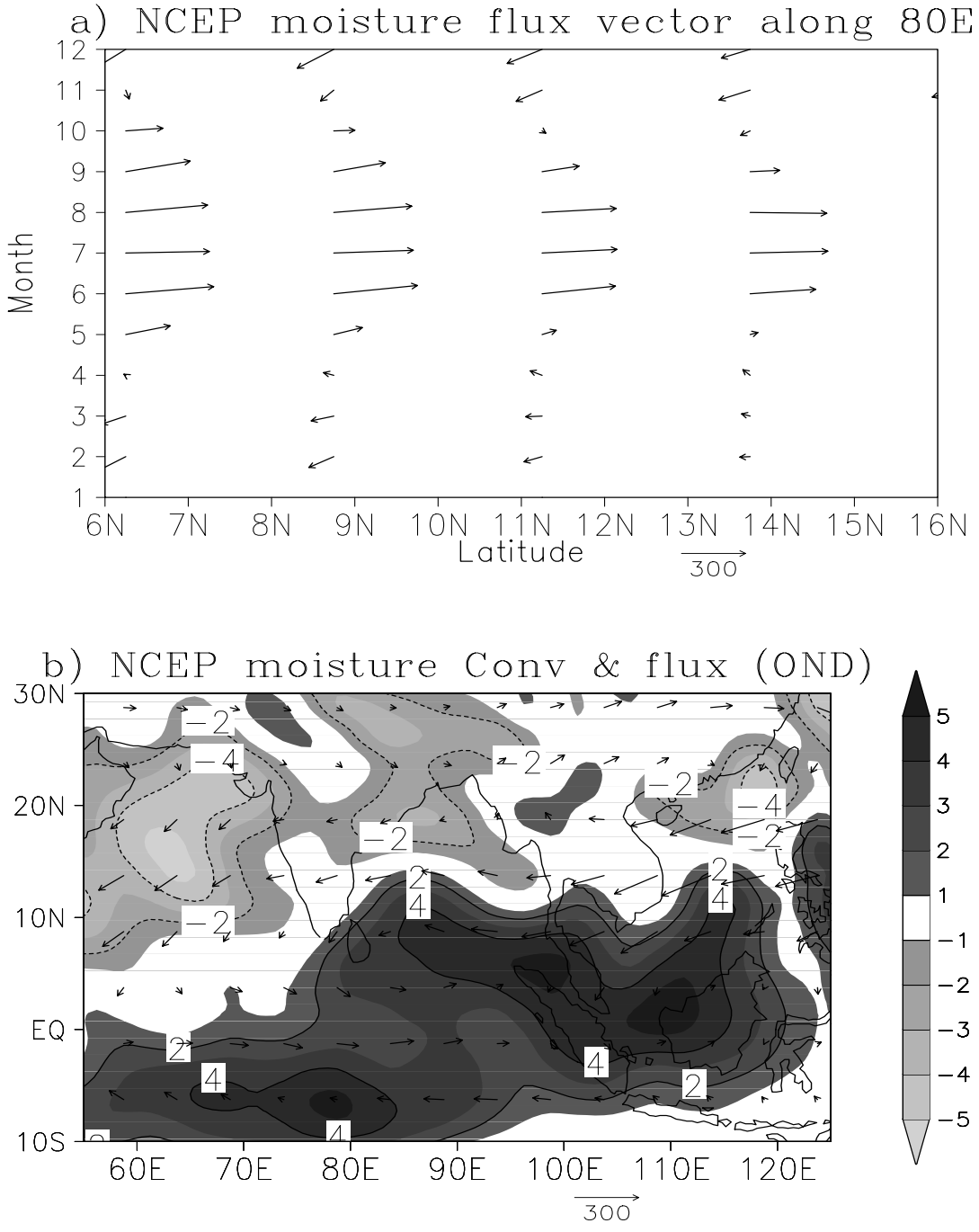

Figure 5.3. Maps of mean moisture convergence and moisture flux over the domain. a) Monthly mean moisture flux for different latitudes along 80E b) spatial pattern of moisture convergence and flux (OND). Positive values are darkly shaded and negative values are lightly shaded]. (Units for convergence: mm/day, moisture flux: kg m^{-1} s^{-1}).

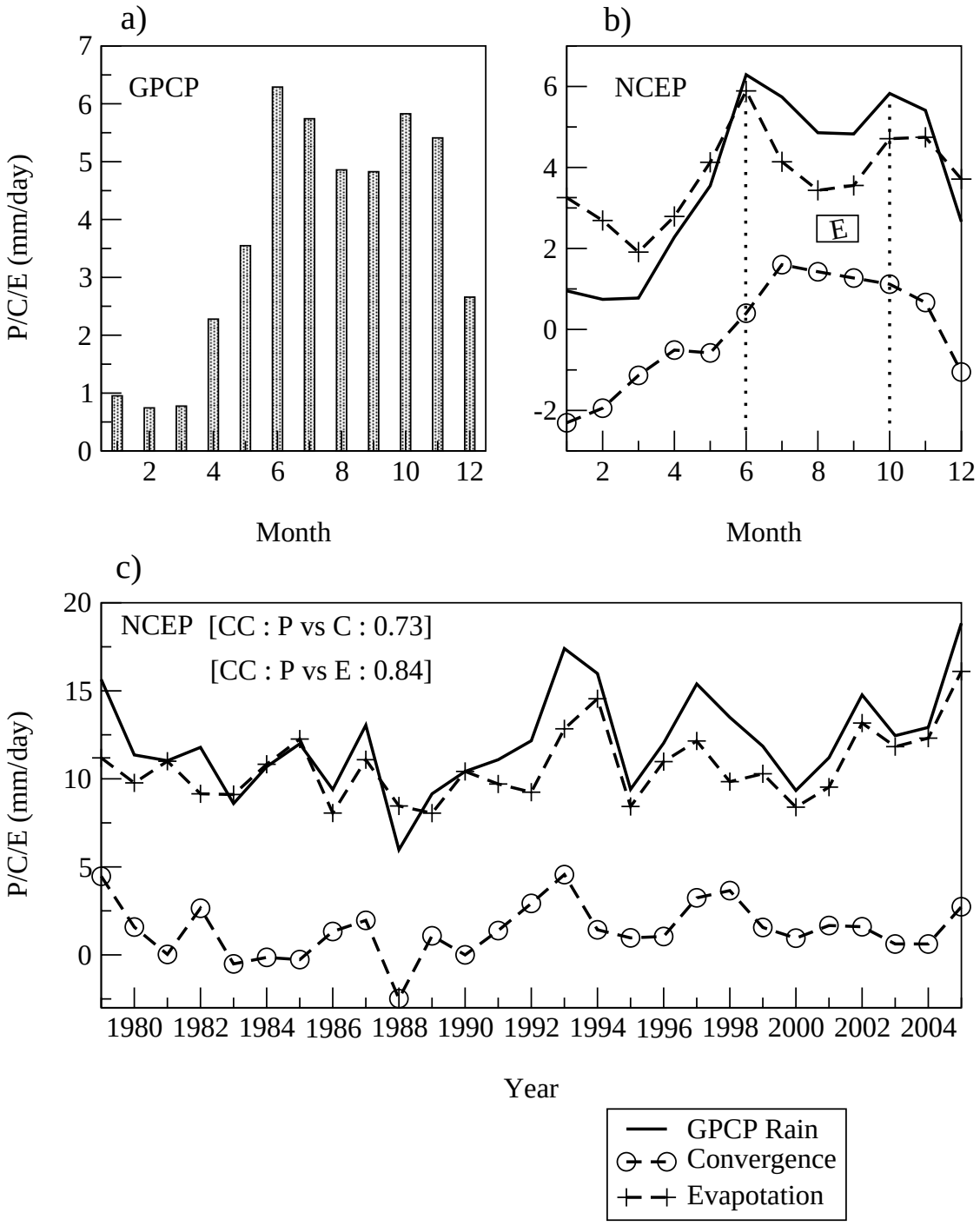

Figure 5.4. Observed monthly mean annual cycle of P, C and E over the selected domain a) GPCP precipitation b) P, C, E (Dominance of evaporation is shown as E in box) and c) Interannual variability of (OND) P, C and E over the selected domain (Value of correlation coefficient between P & C and P& E are shown in graph)

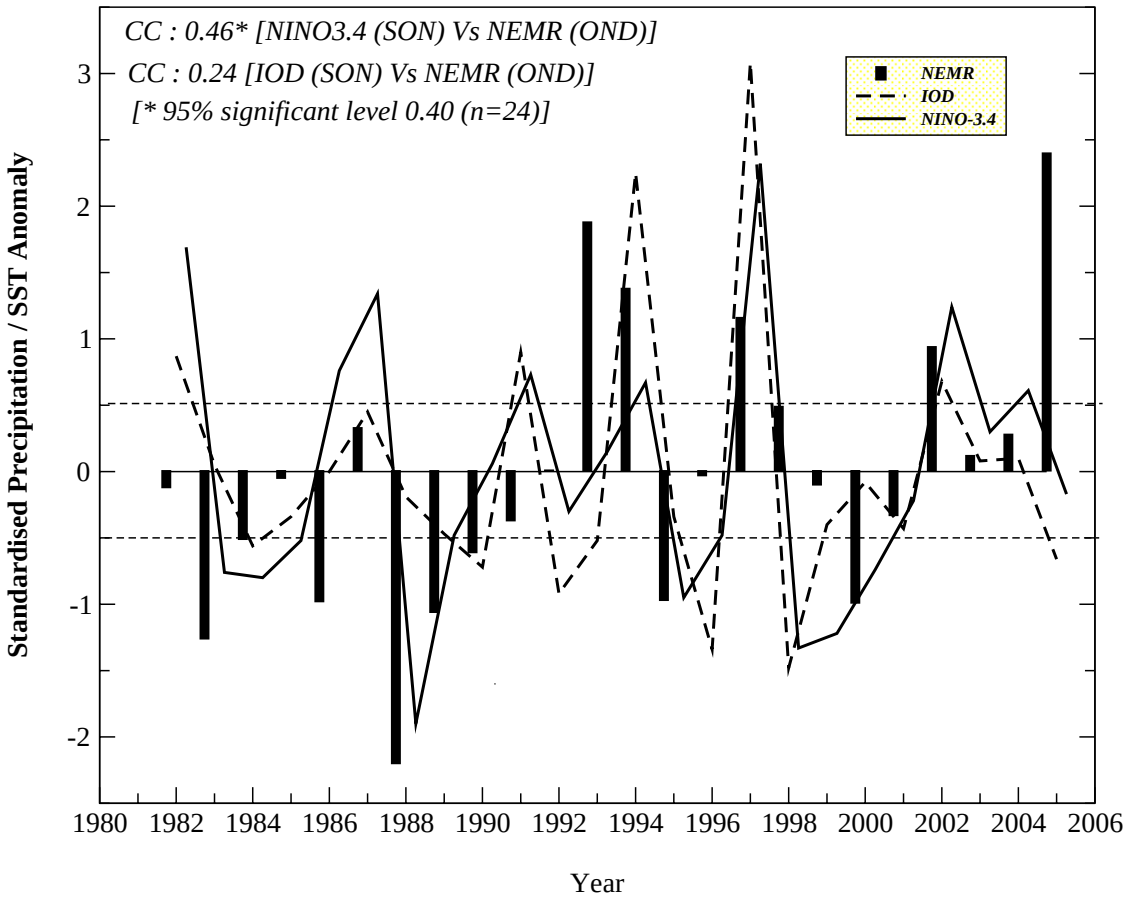

Figure 5.5. Standardised departures of monsoon rainfall over the selected domain (PEN & SL) during (OND), IOD (SON) and NINO-3.4 (SON) anomalies from 1982-2000. (Filled bars denote rainfall departures and dashed line denote IOD index and solid line denote Nino-3.4 anomalies. 0.5 standardised anomaly level is shown by horizontal dashed lines).

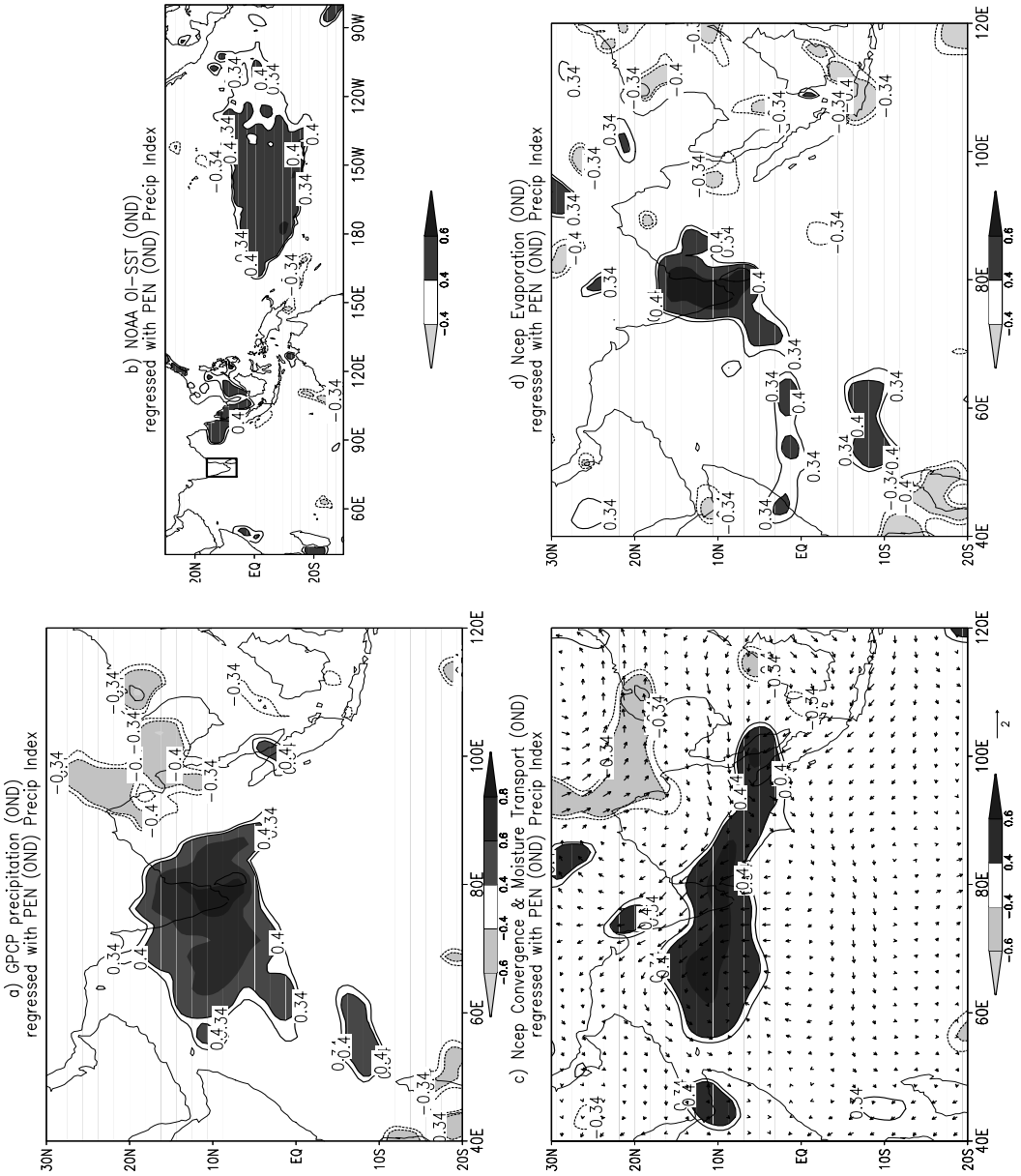

Figure 5.6. Regression maps based on (PEN&SL) domain GPCP precipitation. (Top Panel) a) GPCP Precipitation, b) OND SST (Domain encompassing PEN & SL is shown by a box). (Lower Panel) c) NCEP moisture convergence and moisture flux transport, d) NCEP evaporation. [95% significant levels are shaded and 90% are just contoured]. (Shades indicate regression coefficient), (Units for precipitation, convergence & evaporation: mm/day, SST: deg C, moisture flux: kg m^{-1} s^{-1}).

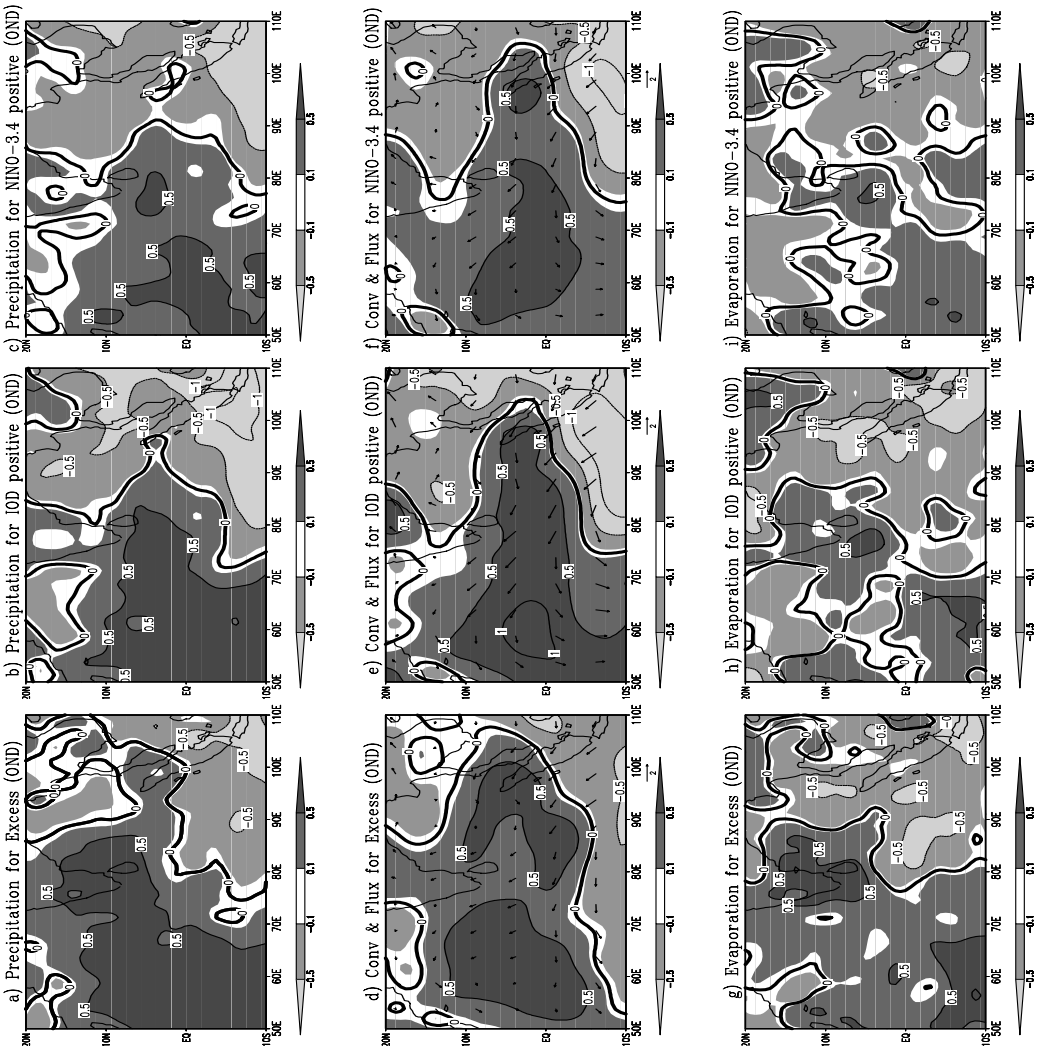

Figure 5.7. Standardised anomaly maps based on Excess and Indian Ocean Dipole Positive Mode Phase and NINO3.4 Positive Anomaly Phase. (Top panel) GPCP Precipitation, a) for Excess year (OND) b) for IOD Positive phase c) for NINO3.4 positive phase. (Middle Panel) moisture convergence and moisture flux transport, d) for excess year e) for IOD positive phase f) for NINO3.4 positive phase. (Bottom Panel) Evaporation, g) for excess year h) for positive phase i) for NINO3.4 positive phase. [Positive anomalies are darkly shaded and negative anomalies are lightly shaded, zero line is shown by a thick line]. (Units for precipitation, convergence & evaporation: mm/day, moisture flux: kg m^{-1} s^{-1}).

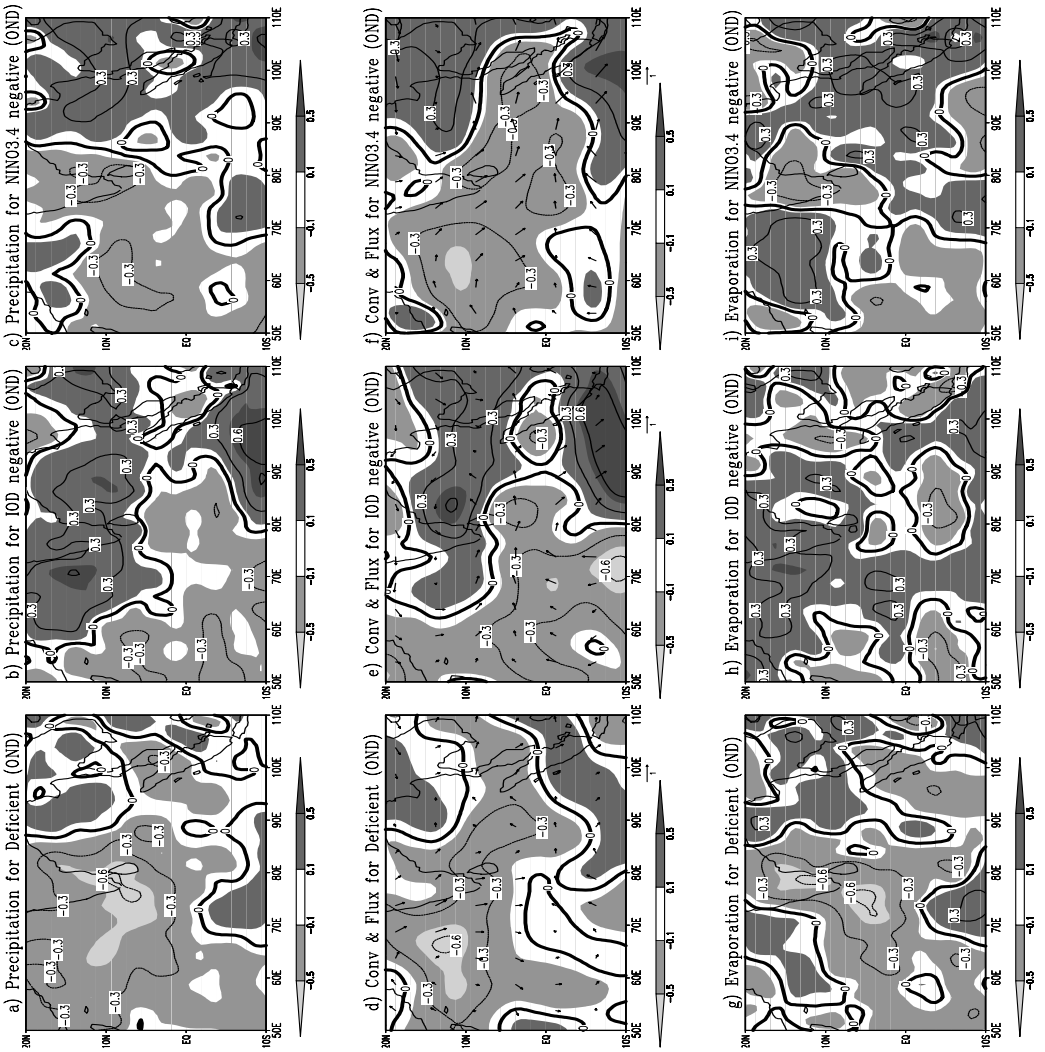

Figure 5.8. Standardised anomaly maps based on deficient and Indian Ocean Dipole negative mode phase and NINO3.4 negative anomaly phase. (Top Panel) GPCP precipitation, a) for deficient year (OND) b) for IOD negative phase c) for NINO3.4 negative phase. (Middle Panel) moisture convergence and moisture flux transport, d) for excess year e) for IOD negative phase f) for NINO3.4 negative phase. (Bottom Panel) Evaporation, g) for deficient year h) for negative phase i) for NINO3.4 negative phase. [Positive anomalies are darkly shaded and negative anomalies are lightly shaded, zero line is shown by a thick line]. (Units for precipitation, convergence & evaporation: mm/day, moisture flux: kg m^{-1} s^{-1}).

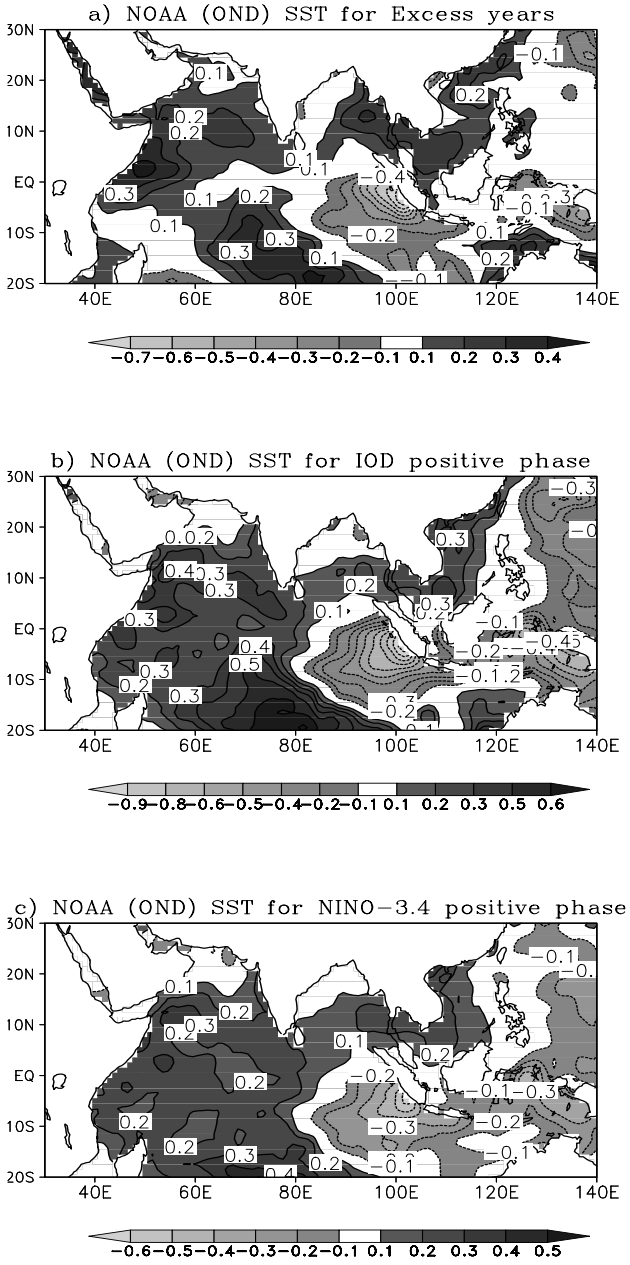

Figure 5.9. NOAA composite SST anomaly maps based on Excess NEMR years, Indian Ocean Dipole positive mode phase and NINO3.4 positive anomaly phase.

(Top Panel) a) for excess years (OND) (Middle Panel) b) for IOD positive phase (Bottom Panel) c) for NINO3.4 positive phase. [Positive anomalies are darkly shaded and negative anomalies are lightly shaded]. (Units for SST anomaly: deg C).

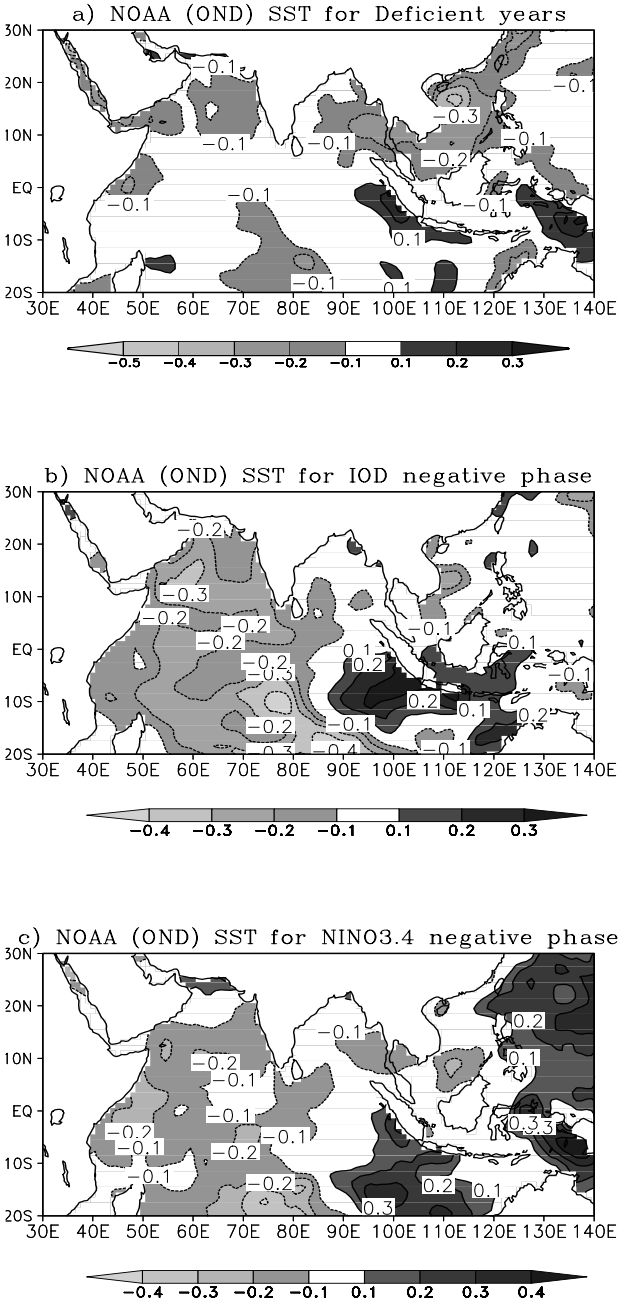

Figure 5.10. NOAA composite SST anomaly maps based on deficient NEMR years, Indian Ocean Dipole negative mode phase and NINO3.4 negative anomaly phase. (Top panel) a) for deficient years (OND) (Middle Panel) b) for IOD negative phase (Bottom Panel) c) for NINO3.4 negative phase. [Positive anomalies are darkly shaded and negative anomalies are lightly shaded]. (Units for SST anomaly: deg C).

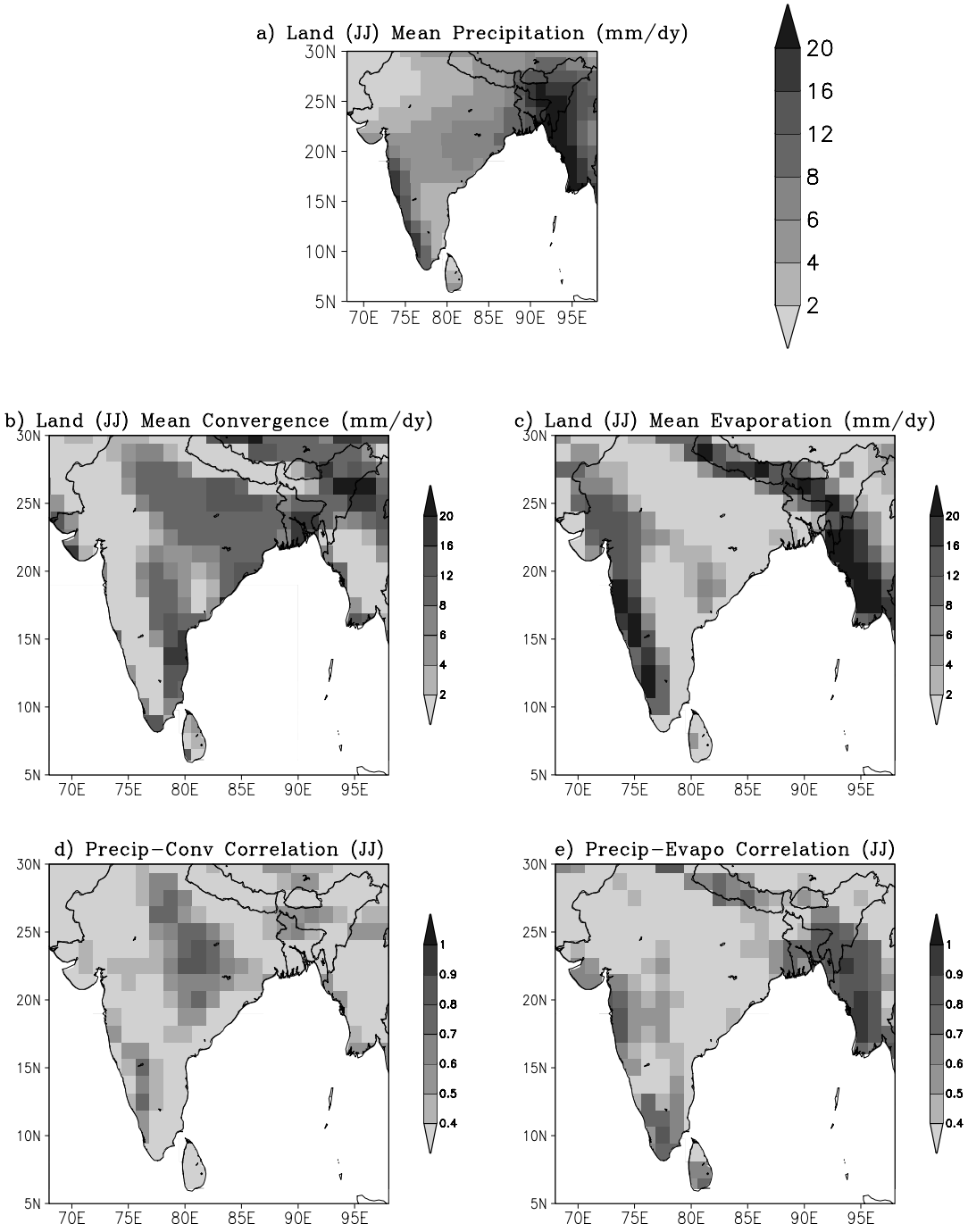

Figure A.1. JRA-25 reanalysis and VASClimO results for early Summer (JJ) season for the period 1979-2000. a) Mean precipitation (P) b) Mean convergence c) Mean evaporation. d) Interannual correlation between (P) and (C) e) Interannual correlation between (P) and (E). (Units for precipitation, convergence & evaporation: mm/day).

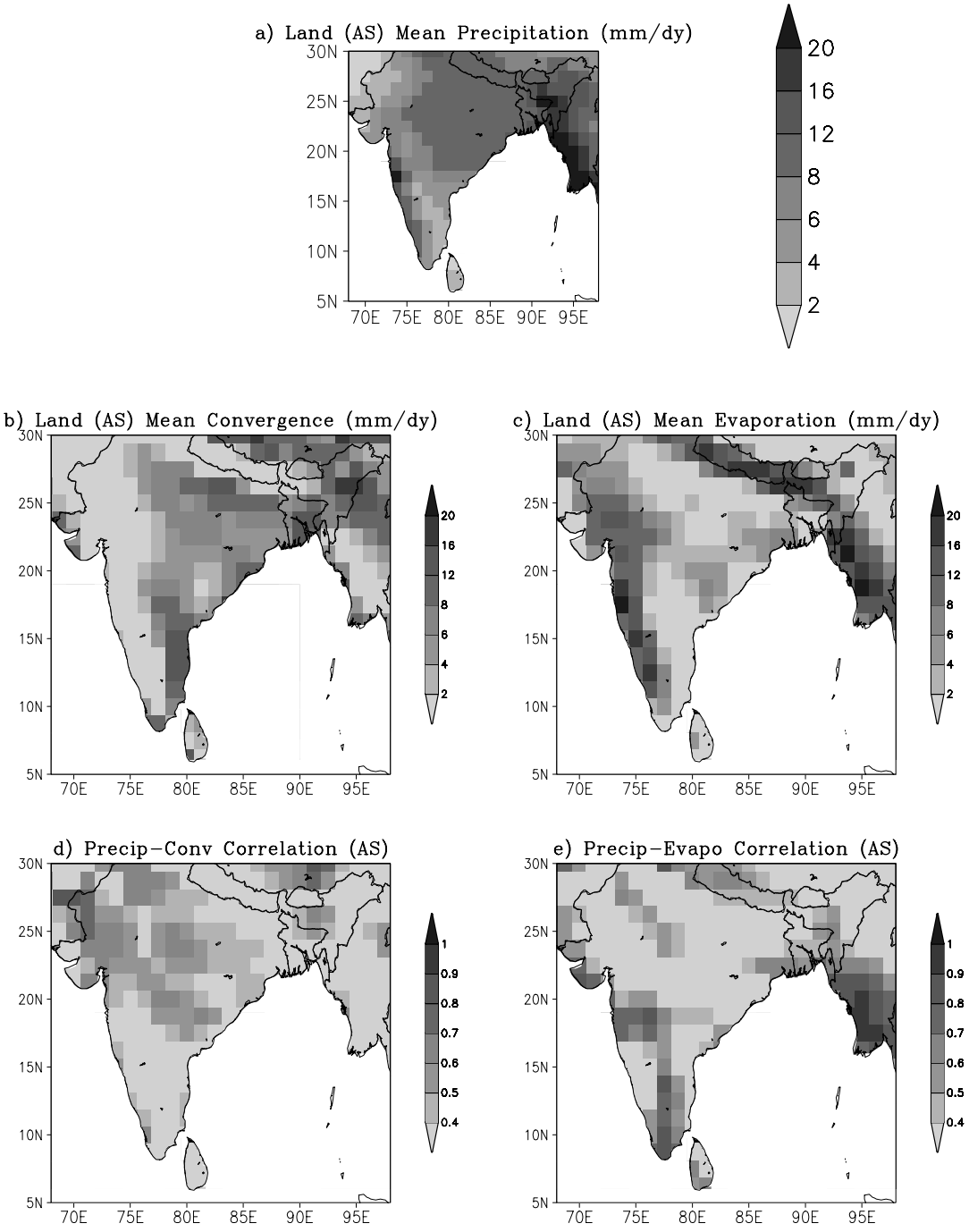

Figure A.2. JRA-25 reanalysis and VASClimO results for late Summer (AS) season for the period 1979-2000. a) Mean precipitation (P) b) Mean convergence c) Mean evaporation. d) Interannual correlation between (P) and (C) e) Interannaul correlation between (P) and (E). (Units for precipitation, convergence & evaporation: mm/day).

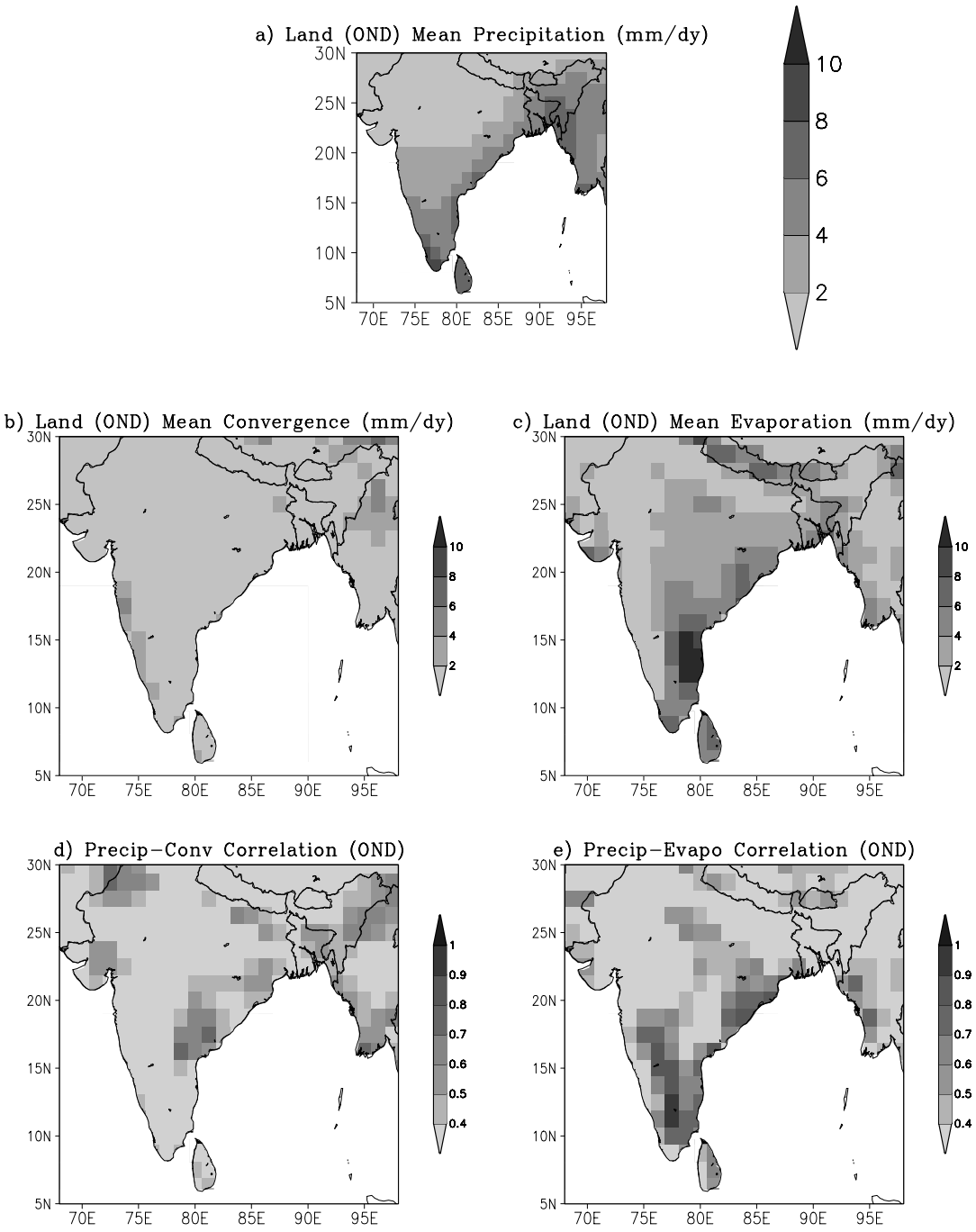

Figure A.3. JRA-25 reanalysis and VASClimO results for NEMR (OND) season for the period 1979-2000. a) Mean precipitation (P) b) Mean convergence c) Mean evaporation. d) Interannual correlation between (P) and (C) e) Interannaul correlation between (P) and (E). (Units for precipitation, convergence & evaporation: mm/day).

TABLES

Table 4.1. Correlation between domain averaged GPCP Precipitation (P) versus domain averaged vertically integrated moisture convergence (C) from three major reanalyses over the South Asian monsoon region. (Bold numerals denote correlation significant at 95% level). (Data Period: 1979-2000)

GPCP (P)	***NWI Domain***	***CEN Domain***	***NEI Domain***	***PEN Domain***	***BOB Domain***	***ARS Domain***	***Season***
							Summer
JRA - 25 (C)	0.86	0.83	0.49	0.46	-0.47	0.41	JJ (Early)
	0.81	0.76	0.54	0.73	0	0.55	AS (Late)
ERA – 40 (C)	0.56	0.68	0.66	0.62	0.26	0.78	JJ (Early)
	0.78	0.68	0.35	0.77	0.57	0.69	AS (Late)
NCEP/ NCAR (C)	0.56	0.64	0.58	0.56	0.3	0.63	JJ (Early)
	0.75	0.74	0.4	0.77	0.02	0.79	AS (Late)

Table 5.1. Selected cases of Excess NEMR, Deficient NEMR, IOD Positive, Negative phases and El Nino, La Nina Phases

Excess NEMR	Deficient NEMR	IOD Positive	IOD Negative	El Nino	La Nina
1993	1983	1982	1984	1982	1983
1994	1984	1991	1990	1986	1984
1997	1986	1994	1992	1987	1985
2002	1988	1997	1993	1991	1988
2005	1989	2002	1996	1994	1995
	1990		1998	1997	1998
	1995		2005	2002	1999
	2000			2004	2000

Data Period: 1979-2005

Table 5.2. Summary of major findings from the study

NEMR Variability	IOD conditions			Nino 3.4 conditions	
	Positive	Negative		El Nino	La Nina
NEMR Positive	Yes	-		Yes	-
i.e., NEMR Positive ~ IOD Positive + El Nino					
NEMR Negative	-	No		-	Yes
i.e., NEMR Negative ~ La Nina (only)					